Tunneling in Warsaw

by
John Hopkins (SID)
Fourth-year undergraduate project in
Group D, 2013/2014

I hereby declare that, except where specifically indicated, the work submitted herein is my own original work.

Signed: John Hopkins Date: 28/5/2014

Technical Abstract

Warsaw Metro Line II is currently nearing the end of the first phase of construction. Analysis of monitoring data acquired during constructing of 7 stations has improved knowledge for the design and implementation of a further 21 stations in similar ground conditions.

Initial research and literature review provided information on the technical aspects of tunneling design in an urban environment, previous knowledge from other tunneling projects, tunneling method implemented, types of monitoring equipment installed, ground conditions and the common soil layers found in Warsaw.

MATLAB was used to process, select, analyse and plot relevant data acquired from the monitoring data dissemination system. A range of techniques were developed to best fit Gaussian curves approximations to real settlement data. The most effective of these sweeps a region surrounding the measured data by varying each of the parameters within the Gaussian curve equation. The best fit is selected from this host of curves by minimising the total horizontal and vertical distances between the curve and the measured data. An investigation into the number of parameter changes to consistently produce the same best-fit curve revealed that 40 were required.

Analysis of transverse settlement on the D10 section of tunnel revealed volume losses and trough width parameters for the various cohesive and non-cohesive soil layers common in Warsaw. Volume losses were found to be between 0.18-0.22% and 0.29-0.35% for cohesive and non-cohesive soils respectively. Trough width parameters were found to be between 0.32-0.4 and 0.27-0.34 for cohesive and non-cohesive soils respectively. Observation of maximum settlement also revealed a learning curve for this section, which through knowledge from this report can be eliminated in the future.

Investigating the under passing of an existing tunnel alongside grouting processes provided a comparison between greenfield, grouted and non-grouted response of ground movements and the existing tunnel movements. Two separate grouting

phases caused heave values of 1.52% and 1.24% of the tunnel face area. Grouting acted to reduce the volume loss by around 20% and increased the width of the settlement trough. Installation of grouting tubes and ground 'relaxation' post grouting were found to produce volume losses of 0.25% and 0.44% respectively.

Building investigations revealed that masonry buildings are fairly flexible for the passing of the first tunnel, but becoming increasingly stiffer as the second tunnel passes and consolidation occurs. These are represented by reductions in modification factors from 0.85 to 0.32 for sagging bending moments for example.

Discussion takes place as to how MATLAB techniques could be developed to further automate the analytical methods of assessing ground movements and building damage criteria. Their feasibility is then discussed for use in real time monitoring.

1 Introduction

1.1 Background

Warsaw is Poland's capital and largest city, with 1.711 million residents, making it the 9th most populous city in Europe. Despite its population its Metro is currently only the 24th busiest in Europe, having carried 139.2 million passengers since Metro Line I opened in 1995. Figure 1-1 shows the existing Metro Line I (blue), consisting of a single north-south connection, linking the city centre with its densely populated northern and southern suburbs. The initial section of the second Metro Line II (red), an east-west line, began construction in August 2010. Scheduled for completion in the summer 2014, this section will be 6.1km long, consisting of 7 stations. Świętokrzyska station will act as a transfer station to the existing Line I and the tunnel will pass under the Vistula River. The primary aim of the Metro Line II is to reduce congestion in the central district, particularly on the bridges crossing the river. "The construction of the central section of Metro line II is the biggest Local-Governmental investment in Poland"(Lejk 2012). This quote, from the Warsaw Metro 2012 Annual Report shows both the size and significance of this investment.

1.2 Motivation

The dotted lines in Figure 1-1 illustrate the primary motivation for this project. As can be seen, there are a further 21 proposed stations to complete the east-west line and a further 3 stations completing the north-south line, omitted from the initial construction due to financial difficulties. Work on Metro Line I progressed very slowly at a speed no greater than 2 metres a day due to lack of funds, poor planning and tedious bureaucracy (Wikipedia 2014). Metro Line II was therefore constructed using the most advanced technology applied to drill tunnels around the world. "This is the first time in Poland when Metro tunnels have been drilled with the use of TBM EPB shields" (Lejk 2012). This is important as "one major difference between geotechnical engineering practices and other civil engineering techniques is that geotechnical engineering requires competent relevant experiences for sound judgments and relatively less dependency on code based design" (Brighthub Engineering 2012). This emphasises the significance of the learning process that takes place through experience of geotechnical engineering practices. This project acts at an opportune stage in the construction of Line II to assess what has happened thus far. Construction of Line II was awarded to the consortium lead by the Italian construction firm Astaldi (Railway-technology.com 2008). Astaldi installed a multitude of measuring equipment to monitor ground movements, detailed in 3.4. Via careful selection and analysis of the measured data much can be learnt about the effects of this tunneling method on grounds movements and specific infrastructure found in Warsaw. With such insight design parameters can be more accurately predicted when planning and implementing further tunneling, providing safer, quicker and more cost effective construction in the future.

1.3 Project Outline

There are 3 areas of investigation that this report will address. The first involves analysing the transverse settlement along the D10 tunnel section, where there is the greatest density of ground pins. The second will investigate the effect of compensation grouting where Line II underpasses the existing Line I. The third involves a comparison between green field settlement and building settlement for a building situated above the tunnel path. These will be achieved by reviewing relevant literature regarding tunnel design, previous tunneling experience in an urban environment, the ground conditions, tunneling procedure and monitoring data systems. A methodology will be devised for analysing specific ground movements using MATLAB to provide data processing techniques and a curve-fitting algorithm. This methodology will be used at different lengths to complete each of the 3 tasks.

1.4 Project Objectives

i. Obtain greater understanding of tunneling in the urban environment, through literature papers, design practice documentation and previous experience.
ii. Gain an understanding of the ground conditions (geological and hydrogeological) specific to Warsaw, namely in the regions to be tunneled.
iii. Develop an efficient approach of obtaining measured data from various monitoring systems.
iv. Devise methods of selecting, processing, analysing and plotting relevant data.
v. Provide Gaussian curve approximations to real settlement data.
vi. Obtain useful parameters from Gaussian approximations for a variety of strata
vii. Investigate the effects of grouting, specifically underneath an existing tunnel.
viii. Investigate building stiffness' as TBM's underpass existing structures.

1.5 Nomenclature

V_L =Volume Loss (%)

TBM = Tunnel Boring Machine

TAM = Tube à Manchette

OC = Overconsolidated

K = Trough Width Parameter

S_{max} = Maximum Settlement (mm)

S_v = Settlement (mm)

y = Horizontal distance from the tunnel centre-line

i = Horizontal distance from tunnel centre to inflexion point of settlement trough

z_0 = Tunnel Depth

EPB = Earth Pressure Balance

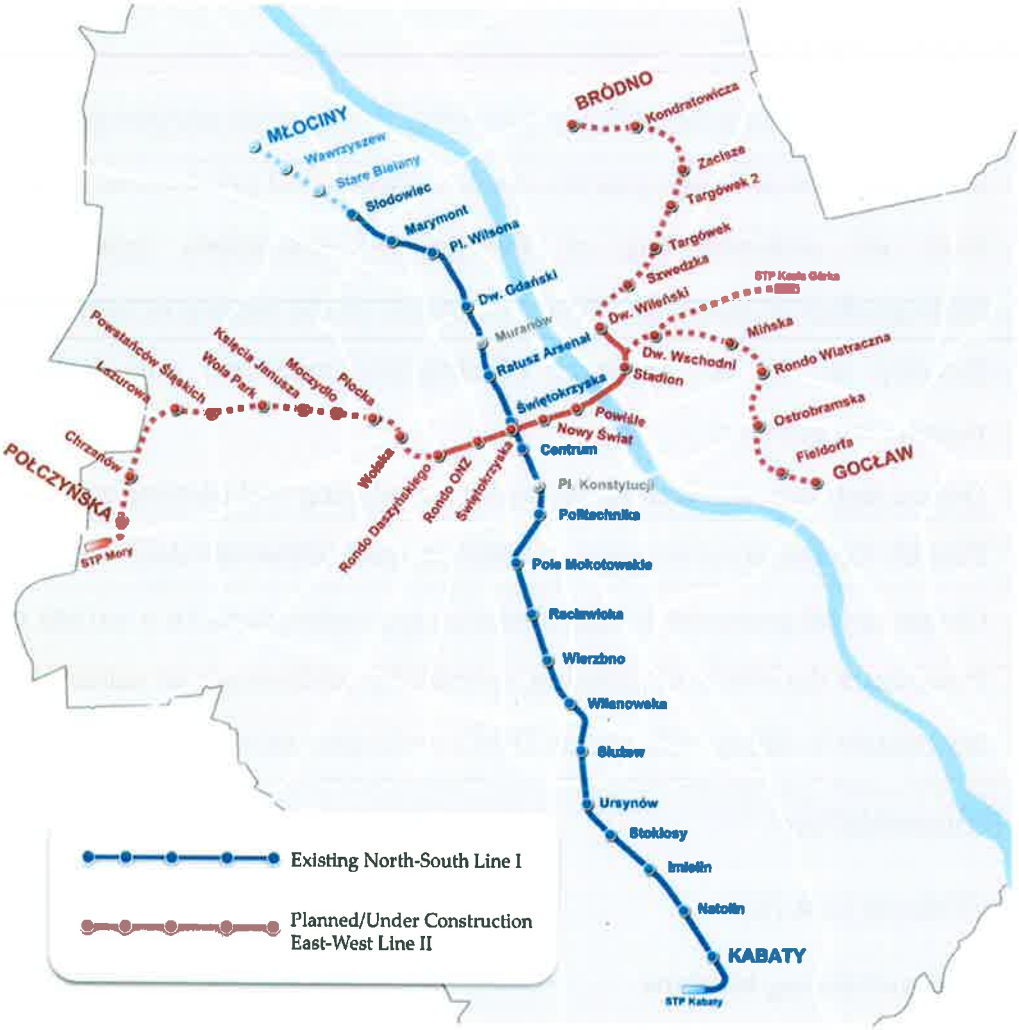

Figure 1-1 - Existing and Planned/Under Construction Metro Lines I and II

Figure 1-2 - Section of Interest

2 Technical Background and Previous Relevant Experience

In order to analyse the data available considerable reading was done surrounding ground movements and their effects due to tunneling and deep excavations. Considering this project is in an urban environment it is essential to have a methodology, which via measured real data can infer useful parameters such as volume loss and trough width factor.

2.1 Gaussian Distribution curve in Green Field Conditions

Ground movements are initially considered for the "green field" case, which are the expected movements for unloaded, undisturbed ground. The development of the surface settlement trough above and ahead of the advancing heading is shown in Figure 2-1. The procedure follows that described by Peck (1969) showing that a settlement trough immediately after a tunnel has been constructed follows a Gaussian distribution curve, described below and illustrated in Figure 2-2.

$$S_v = S_{max} \exp \frac{-y^2}{2i^2} \tag{2.1}$$

2.2 Volume Loss

Volume loss is an important parameter in tunneling, commonly based on engineering judgement and experience from previous projects in similar ground using similar techniques (Macklin, 1999). It depends predominantly on the type of ground and the tunneling method such that a site investigation and an assumed volume loss can provide useful parameters for construction such as face support pressures. The term itself is expressed as a percentage ratio between the volume of the surface settlement trough V_s (per metre length of tunnel) and the excavated area of the tunnel, expressed as follows

$$V_s = V_l \frac{\pi D^2}{4} \tag{2.2}$$

V_s is found by integrating equation 2.1 to obtain

$$V_s = \sqrt{2\pi} i S_{max} \tag{2.3}$$

2.3 Trough Width Parameter K

It is clear from equation 2.1 that the parameters affecting the shape of the settlement trough are S_{max} and i. O'Reilly and New (1982) investigated UK tunneling data to show that i varies approximately linearly with tunnel depth z_0 and is independent of construction method and tunnel diameter. It is therefore defined by

$$i = Kz_0 \tag{2.3}$$

For practical purposes they recommend taking K to be 0.5 for tunnels in clays and 0.25 in sands.

2.4 Building Stiffness

The stiffness of a building will determine how similar the settlement profile is beneath the building to that of the green field. It is commonly assumed that the building is separated into hogging and sagging zones, each zone is treated as if they are separate buildings (Mair 2013) with a deflection ratio per zone as defined in Figure 2-3. The stiffness is then represented by a modification factor; the ratio of the deflection ratio experienced by the building, $DR_{hog\ or\ sag}$ and the deflection ratio for the green field case, $DR^{gf}{}_{hog\ or\ sag}$. These are calculated and plotted against relative building stiffness $\rho_{sag\ or\ hog}$ to see if they fit within a design envelope (Figure 5-18)

2.5 Figures

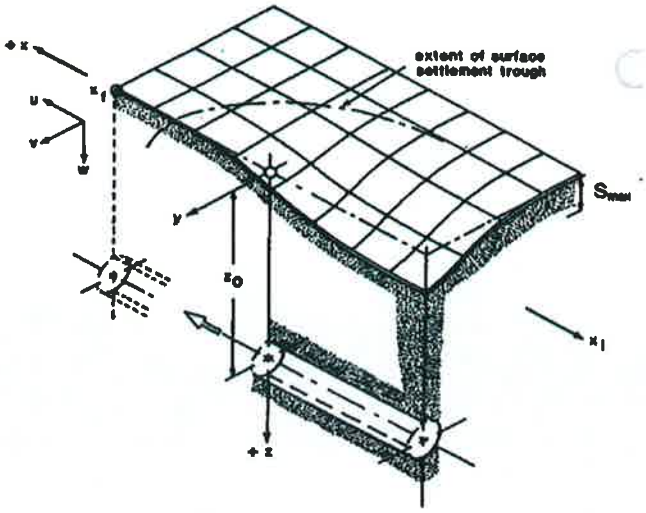

Figure 2-1 - Settlement above advancing tunnel (Attewell et al, 1986)

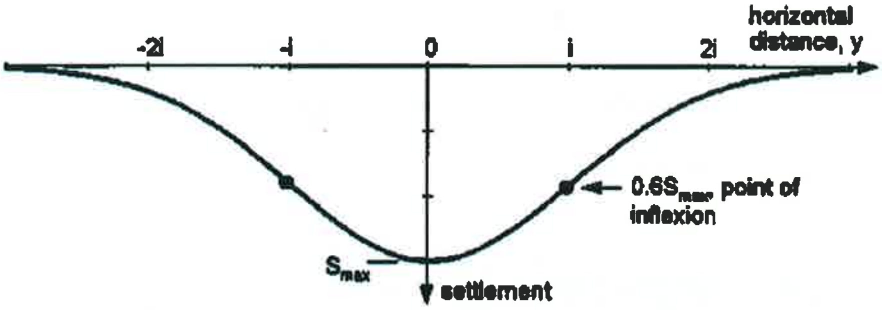

Figure 2-2 - Gaussian Curve for a Settlement Trough (Mair, Taylor and Burland, 1996)

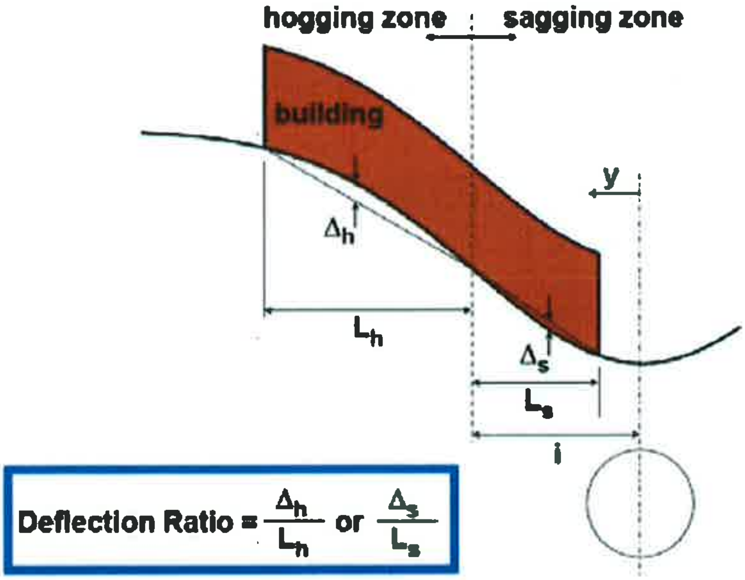

Figure 2-3 - Deformation of a building above a tunnel (Mair et al, 1996)

3 Site Conditions and Measurement Data

3.1 Tunnel Section of Interest

This report is concerned with tunnel sections D10, D11, D12 and D13 and stations C9, C10, C11, C12 and C13, situated west of the river (red line in Figure 1-1). This section can be seen in plan below in Figure 3-1 and in cross section in Figure 3-2.

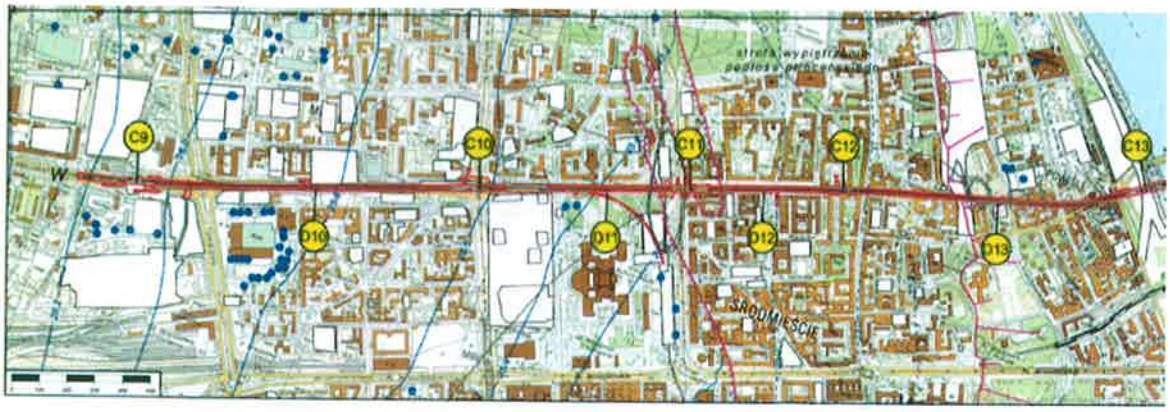

Figure 3-1 - Plan view of Tunnel from Station C9 to C13

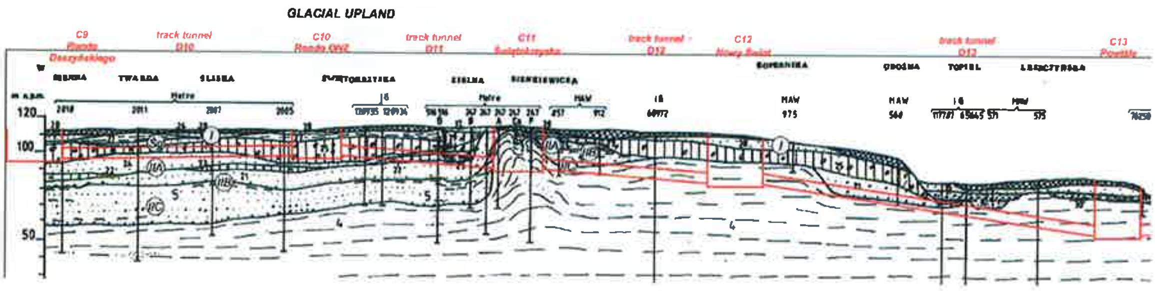

Figure 3-2 - Cross Section of Tunnel from C9 to C13

3.2 Ground Conditions

3.2.1 Site investigation

An extensive site investigation was carried out for the AGP Metro Polska Civil Partnership by GEOTEKO Geotechnical Consultants Ltd. The subsoil is made up of a 1-3m thick fill layer (locally up to 8m in some places) underlain by alternating layers of fluvioglacial, limnoglacial and moraine soils of Warta and Odra Glaciations. The sandy deposits (fluvioglacial and limnoglacial) are represented by soils of different grain-size distribution from fine to medium sands with admixture of gravels and pebbles. The cohesive soils (limnoglacial and moraine) are represented by silts, sandy silts and clays, sandy clays and more plastic sandy clays, with an admixture of gravels and pebbles. The glacial deposits are underlain by a continuous layer of mazovian interglacial and pre-glacial deposits consisting of sands of different grain-size from silty to medium sands, with an admixture of gravels. The water table is found between 25 and 26m above the Vistula River with natural variations of ±0.3m. It is predicted that hydrostatic pressure deformations will be relatively small compared to the natural variations of groundwater level. High permeability parameters of the aquifer, location of the tunnel parallel to the current lines (all except Line I crossing) and its small interface with water bearing layers will in practice, cause no deformation of groundwater flow (Geoteko Geotechnical Consultants Ltd., 2010).

3.2.2 Geotechnical Identification

16 geotechnical layers were identified in the subsoil. They are marked from I to VIII with additional selections marked a, b and c. These layers are categorised as follows.

3.2.2.1 Tertiary soils (Layer I)

Of Pliocene origin, created during sedimentation of weathered material transferred to inland reservoirs and periodically dried. Their grain-size distribution consists of: Ia - high plasticity clays, silty high plasticity clays, more plastic clays; Ib - other cohesive soils, mainly silty clays and silts; Ic – sands of different grain-size distribution, namely silty and fine sands.

3.2.2.2 Quaternary soils (Layers II-VII)

Created in the processes of accumulation and denudation of the subsequent transitions of continental glacier. These are subdivided into non-cohesive (Layers II, III and IV), cohesive (Layers V and VI) and increased organic matter (VII).

- Non-Cohesive soils are categorised by both grain-size and density into:
  - Layer II - Fine and silty sands
    - IIa - Sands only of river terraces of $I_D < 0.4$
    - IIb - Sands of $0.4 < I_D < 0.7$
    - IIc - Sands of $I_D > 0.7$
  - Layer III - Medium and Coarse sands
    - IIIa - Sands of $I_D < 0.7$
    - IIIb - Sands of $I_D > 0.7$
  - Layer IV - Dense sand-gravel mixtures and gravels
- Cohesive soils are categorised by grain-size into:
  - Layer V - Clays
    - Va - Clays, sandy clays of $I_P < 0.2$ and $I_L > 0.25$
    - Vb - Clays, sandy clays of $I_P < 0.2$ and $I_L < 0.25$
    - Vc - More plastic clays of $I_P > 0.2$
- The organic soils consist of sandy muds (VIIa) and clayey muds (VIIb).

The above division criteria allow for the evaluation of geotechnical parameters at positions along the tunnel's cross-section. Identification of soil types for planned future tunnel cross sections will enable the discoveries made in this report to be used when predicting ground movements and identifying design parameters.

3.2.2.3 Anthropogenic fills (Layer VIII)

Urban processes, largely connected to the huge war damages during the Second World War, generated these. These typically occupy the first 1-3m below the surface. Geotechnical parameters are less important in these soils as tunneling will not occur within this region, however we might be interested in their unit weights as they will act as surcharge when undertaking soil stability calculations.

Geoteko Geotechnical Consultants Ltd., 2010 provide more detailed descriptions of each soil sub-layer in their documentation, see References.

3.2.3 Summary of Geotechnical Parameters

Geotechnical parameters for soil subdivisions are provided by ROCKSOIL and are summarised below in Table 1. Of course there is large generalization of geotechnical conditions when stating these values, especially in regions of large heterogeneity.

Soil Type	Unit Weight (kN/m^3)	Drained Shear Strength (kPa)	Friction Angle (°)	Soil Stiffness E (MPa)
Anthropogenic fills	18	5	28	16
Organic Soils	16	5	28	15
Medium and coarse sands, gravels	20.9	0	41	17.2+3.1z
Quaternary cohesive soils	21	5	31	17.3+1.5z
Pliocene cohesive soils	20.6	10	20	22+2.65z
Fine and silty sands	20.3	0	37	17+2.7z

Table 1 - Summary of Geotechnical Parameters

3.3 Tunnel Construction Information

Tunnel Construction began at station C9, heading eastwards with 2 Tunnel Boring Machines (TBMs). Shield 1, named Anna (S-645) began drilling the southern tunnel on 16 May 2012. Shield 2, named Maria (S-644) began drilling the northern tunnel on 18 June 2012. The machines are earth pressure shields, manufactured by Herrenknecht with an outer diameter of 6.27m and a face area of 30.88m^2. Once drilled the tunnel was lined with 1.5m reinforced concrete segments.

3.4 Measurement Data

The biggest enabler of this project is the wealth of data available from a large range of measuring equipment installed along Line II. Having visited Geotechnic Consulting Group (GCG) early on in the project access was provided to DDS' monitoring data dissemination system (Ddsmonitoring.com, n.d). This provided installation sheets and monitoring data for the duration of the construction to date. Clearly not every piece of data would be relevant so careful consideration both geographically and chronologically would be required to isolate the useful data. Data related to the TBMs was also provided via IRIS tunnel system. This consisted of accurate chainage data as well as bearing information as the tunnel progressed.

3.4.1 Ground Pins

These are small metal pins installed in the ground prior to tunneling. Measurement of change in vertical displacement is taken manually periodically using total stations. The significant time required taking a set of ground pin readings means there are only around 50 readings per set of pins, with more frequent readings being taken during significant periods, like when the TBM is passing underneath. Figure 3-3 shows the layout of pins along the D10 section, whilst Figure 3-4 shows a cross section of one set of pins in relation to the tunnel axes. A photograph of one at installation is included in Figure 3-5.

Figure 3-3 - Ground Pin Layout for D10 Tunnel Section

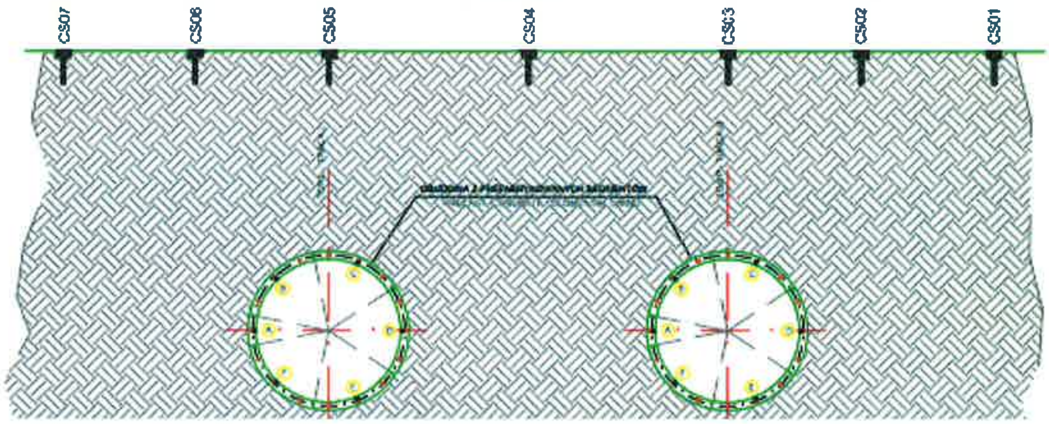

Figure 3-4 - Tunnel Cross Section Showing Ground Pin Layout

3.4.2 Mini Prisms

These are reflective targets positioned strategically such that data can be collected automatically by use of a digital monitoring sensor. The sensors used on this project are Leica TM30s, which have an accuracy of 0.6mm and can readings up to two times every second (Leica-geosystems.co.uk, 2010). There are a number of benefits of mini prisms over ground pins. They are used where movement in 3 dimensions is desired. They can be positioned in challenging places that can be read by an electronic device but would be difficult to take a manual reading. Finally automation enables substantially more frequent data to be taken, providing a more detailed picture of the movements incurred during and post construction. Figure 3-5 shows photographs of a ground pin and two mini prisms being installed on a road, in the existing Line 1 tunnel and on a building respectively

Figure 3-5 - Ground Pin and Mini Prism Installation Photographs

3.5 Grouting Process

One of the largest concerns when constructing line II was under passing line I, whilst keeping Line I fully active. Figure 3-6 shows the region where the tunnels cross one another and the regions to be grouted.

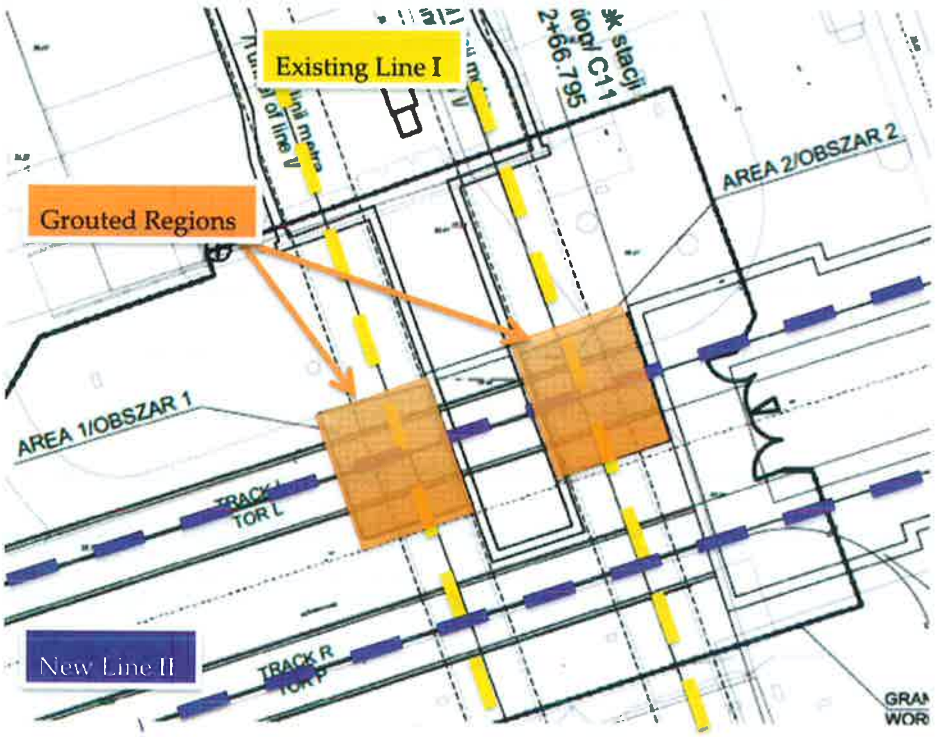

Figure 3-6 - Plan View of Grouting Schematic

Analysis of the geological and geotechnical data shows heterogeneous soil conditions, with cohesive and non-cohesive soils within the area in question. Figure 3-7 and Figure 3-8 show the grouting schematics in section.

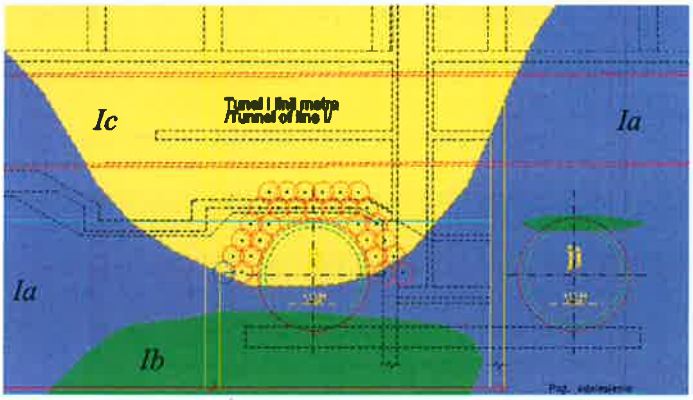

Figure 3-7 – Line II Section Grouting Schematic

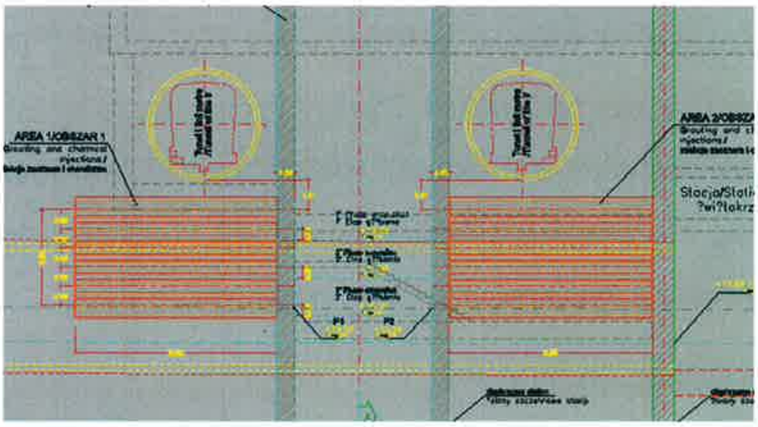

Figure 3-8 - Line I Section Grouting Schematic

As you can see, only the northern tunnel is grouted as it is overlain by OC non-cohesive tertiary soil (Ic) consisting of mainly fine and silty sands. These soils should be treated as impermeable, with a coefficient of permeability $k=10^{-6}$-10^{-4} m/s, therefore their drained shear strength is activated which is negligible for fine and silty sands (Table 1). The southern tunnel is found in OC tertiary cohesive soil (Ia) developed mainly as high plasticity clays ,which are stiff, very stiff and hard. They can be treated in practice as impermeable with coefficient of permeability $k<10^{-9}$ m/s. It was therefore concluded that this soil was both strong and stiff enough (56.45MPa according to Table 1) to not require soil improvement via grouting.

The purpose of the injections "in pressure" is to carry out a soil improvement, in non-cohesive ground, around the future tunnel lining, in order to mitigate the excavation effects on the existing tunnels during the passage of the northern TBM. The low pressure grouting injections took place involved drilling and installing steel casings, inserting injection pipes into those casings, executing sheat grouting, removing steel casing, grout injection and finally chemical injection. Figure 3-8 shows a Line I section view showing that horizontal injections were executed from a shaft excavated between the two existing tracks. The highlighted areas in Figure 3-6 show two areas of approximately 9.5x11m in plan and 4.5m in height, consisting of two rows of horizontal columns.

The exact materials used in the sheat grout, regular grout and chemical mixture can be found in section 5 of Cassani and Stanczyk's report, 2012. During grouting significant monitoring was undertaken. The key parameters to monitor are pressure (current, average, maximum and refusal), volume injected, and instantaneous flow rate. Once drilling was complete a drilling survey was undertaken consisting of two cores through the whole thickness of the improved layer.

3.6 Data Processing Techniques

DDS monitoring provided a useful feature where data for a specific piece of equipment could be exported in its entirety in a .csv file (comma spaced variable). This could be opened in Microsoft Excel but wasn't particularly accessible as individual data entries were not separated into cells. I therefore devised an algorithm within MATLAB, which took the .csv file, separated the entries and assigned general pin information to each one.

Given the time dependent nature of the settlement the most useful plot to represent the data globally was a time versus settlement plot for each set of ground pins or mini prisms, such as Figure 3-9. Labeled on this plot are the two significant changes in settlement caused by the southern and northern tunnels respectively. Taking data from the points labeled 1, 2 and 3, subtracting 1 from 2 and 2 from 3 isolates the settlement due to the passing of each tunnel, essential for later analysis. The last set of points labeled 4 is relevant as it gives an indication of what the consolidated tunnel settlement might be. This will be useful in section 5.3 where final settlement is required to quantify deflection ratios.

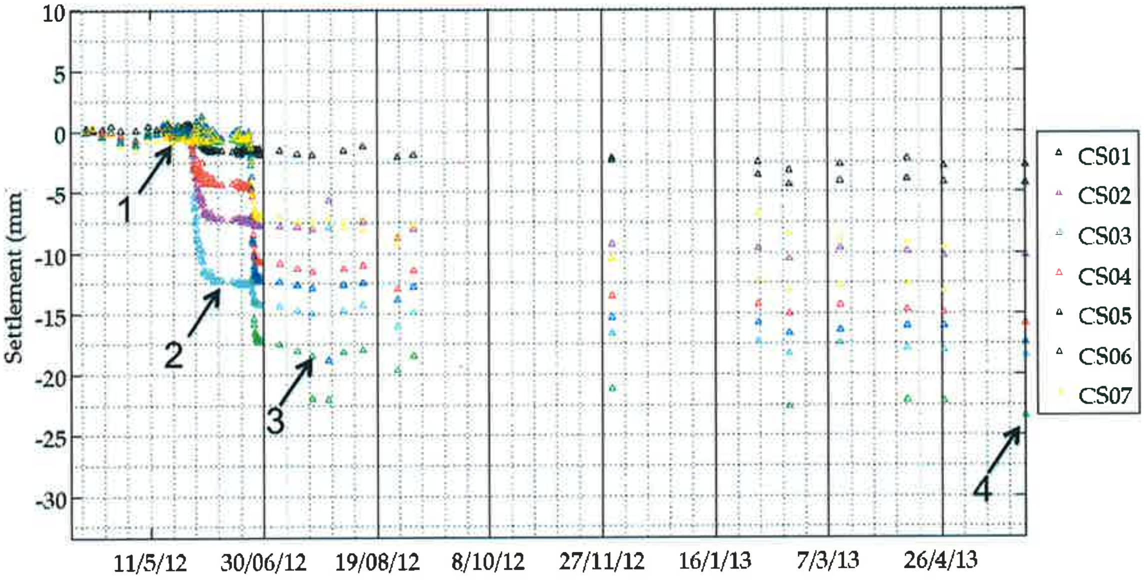

1. Settlement Prior to TBM Arrival
2. Settlement Due to South Tunnel Passing

3. Settlement Due to North Tunnel Passing
4. Consolidated Settlement

Figure 3-9 - Settlement Versus Time for a Standard Ground Pin Set

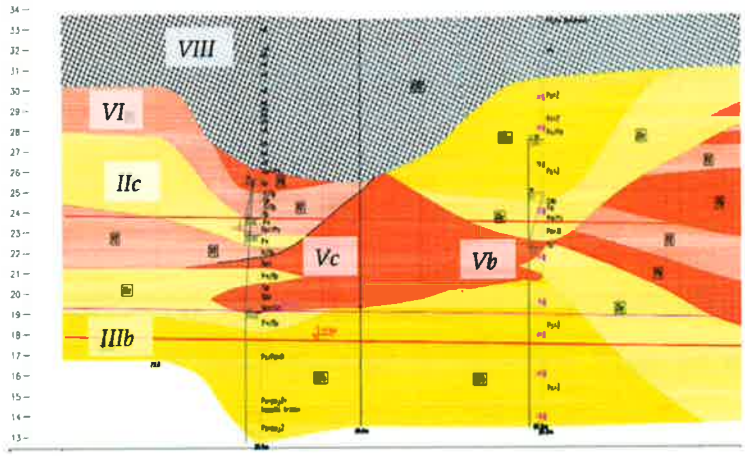

Label	Description
IIa	Fine and Silty Sands (Low Density)
IIb	Fine and Silty Sands (Medium Density)
IIc	Fine and Silty Sands (High Density)
IIIb	Medium and Coarse Sands
Vb	Sandy Clays and Clays
Vc	Plastic Silty Clays and Silty Clays
VI	Clayey Sands and Silts
VIIb	Clays with Organic Matter
VIII	Anthropogenic Fills

Figure 3-10 - Typical Geotechnical Cross Section at the Start of D10

4 Gaussian Approximation Techniques

The output data from the processing in section 3.6 is a series of raw data sets, representative of the Gaussian curves described in section 2.1. The next step is to provide a method of best fitting a Gaussian curve to this data.

4.1 Approximation Techniques

4.1.1 Trapezium Rule Method

This approach involved connecting data points using straight lines and using the mean settlement for each pair of adjacent points to calculate V_S. The justification for this method was that if it provided a reasonable estimate of volume loss then this along with S_{max} would enable Gaussian curve to be plotted, centered on the data point that S_{max} belongs to. Rearranging equation 2.1 would reveal an i value, which via equation 2.4 produces a trough width parameter K.

For values of K around 0.5 this method proved to be fairly reliable. This was justified by sight in that the Gaussian curve appeared to well represent the data points. However for values of K nearer to 0 or 1 the curve approximations were either too thin or too wide respectively. This was due to unequal portions of the curve lying above and below the straight-line trapezium approximations for these K values, leading to erroneous volume losses. As values of K~0.35 are expected for sands (Mair, 2013) this idea was dismissed in search of one more accurate for a wider range of K values.

4.1.2 Manual Approach

This approach involved manually varying K to achieve a best-fit approximation, again based on which estimate by sight, appeared to best represent the measured data. The 'solve' function was used in which Excel incrementally varied K whilst minimising the parameter d. This parameter d is the sum of the horizontal and vertical distances between the curve and the measured settlement at the across track distances of the measured data. This method was effective and provided K values to 3 decimal places, at least enough accuracy given the tolerances of ground pin readings of ±0.25mm (Whalen, 1979). The drawback of this method is the assumption that S_{max} is the maximum measured settlement occurring at its respective across track distance. Given that the ground pins are generally installed above the tunnel axis the assumptions should be valid, however the interference of buildings, other tunnels and grouting may prove this assumption invalid. It is also a time consuming process individually sorting data sets in Excel to enable the function to be run.

4.1.3 K, Smax and H Variation Approach

The 'solve' function is a powerful tool but it is only capable of varying one input variable at a time. This method involves varying 3 input variables so a more powerful computation tool than Excel was required, such as MATLAB. Considering equation 2.1 it is clear that S_v is dependent on S_{max}, y and i. An algorithm was created which varied K (directly affecting i via fixed tunnel depth z_0), S_{max} and H (a variable that acts on y, translating the curve horizontally) one at a time. For each variation a value of d was calculated according to $d = \sum_1^{14} d_i$ where d_1 and d_2 are the horizontal and vertical distances from the approximation curve to the first data point etc. As before, the variation with the smallest d value was selected as the best-fit approximation. Figure 4-1 shows these variations, separating variables by colour with the raw data and best-fit curve shown in blue and magenta respectively.

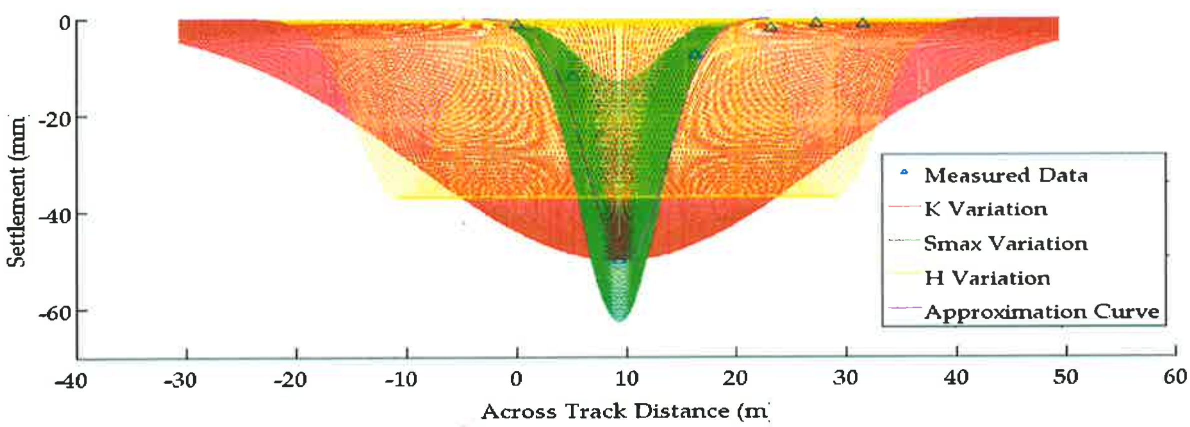

Figure 4-1 - Plot to Demonstrate K, Smax and H Variation

Tests were done on the same data set for the 6 arrangements of variation change to determine which provided the lowest d value, resulting in the most successful order being the one chosen to title this section, varying K, followed by S_{max}, followed by H. This method was again effective and calculated some very good approximations. However it too ran into some difficulty coping with the external factors mentioned in 4.1.2. These arose as varying K first meant selecting initial values of S_{max} and H, which meant on occasion the best-fit curve would not be located as different initial values of S_{max} and H to begin with would've yielded a different, better result.

4.1.4 Sweep Technique

This final approach varied the same 3 variables as in 4.1.3 but rather than varying K N times, followed by S_{max} N times, followed by H N times it varied all S_{max} and H combinations for each K value and so on. This is represented by the embedded 'for loops' in the MATLAB code extract in Figure 4-2.

```
nosamples=N;
for j1=1:nosamples
   for j2=1:nosamples
      for j3=1:nosamples
         finalsweep;
         count=count+1;
      end
   end
end
```

Figure 4-2 - Code Extract from MATLAB Sweep Algorithm

This provides a thorough sweep of the region surrounding the measured data. The primary concern with this method is that to provide a better approximation requires increasing the number of samples N. As the run time for the program scales with N^3 this quickly leads to significant run times as N increases.

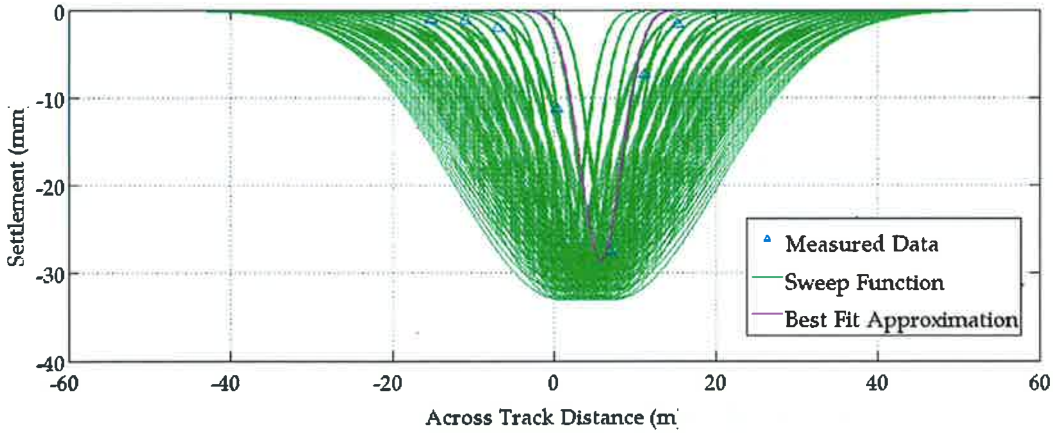

Figure 4-3 - Sweep Technique with N=5

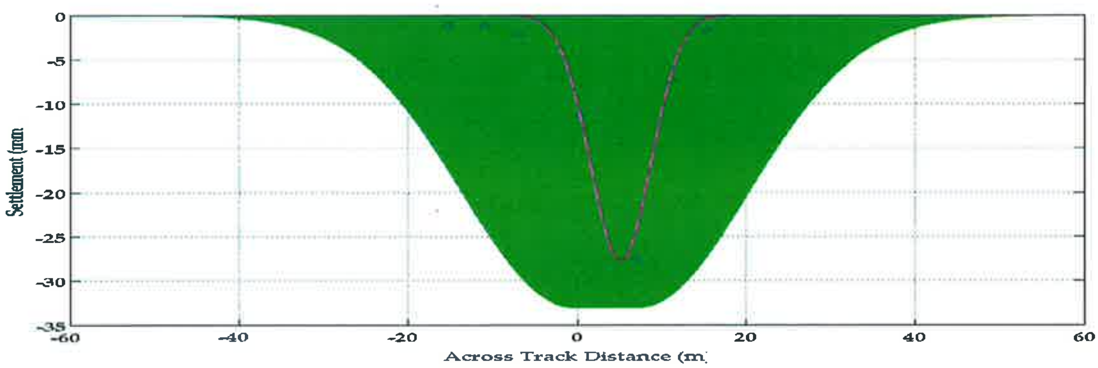

Figure 4-4 - Sweep Technique with N=40

Figure 4-3 and Figure 4-4 show this sweep technique with N=5 and N=40 respectively. It can be clearly seen that N=40 produces a finer sweep and a closer approximation curve however the run times were 2.65 and 266.9 seconds respectively. This significant increase in run time, so it is evident there will have to be some form of compromise between accuracy of best-fit curve and run time to make this technique practical.

4.2 Proof of Concept

To provide justification for this technique the algorithm was run for a range of N values with 6 sets of data representing the passing of the northern and southern tunnels underneath 3 sets of ground pins. N values were varied between 2-100 with a total runtime of 3 hours 40 minutes. Key Parameters V_L, K and Smax are plotted against number of samples N in Figures 4-5, 4-6 and 4-7. It can be clearly seen that the parameters vary significantly below N=10, but beyond N=40 the variables converge on the best fit, with only small fluctuations as N increases. To carry out a sweep with N=40 (not plotting the every sweep curve like in Figure 4-4) takes around 30 seconds, an acceptable run time, so this value will be used to provide the best-fit approximations in the investigations in section 5.

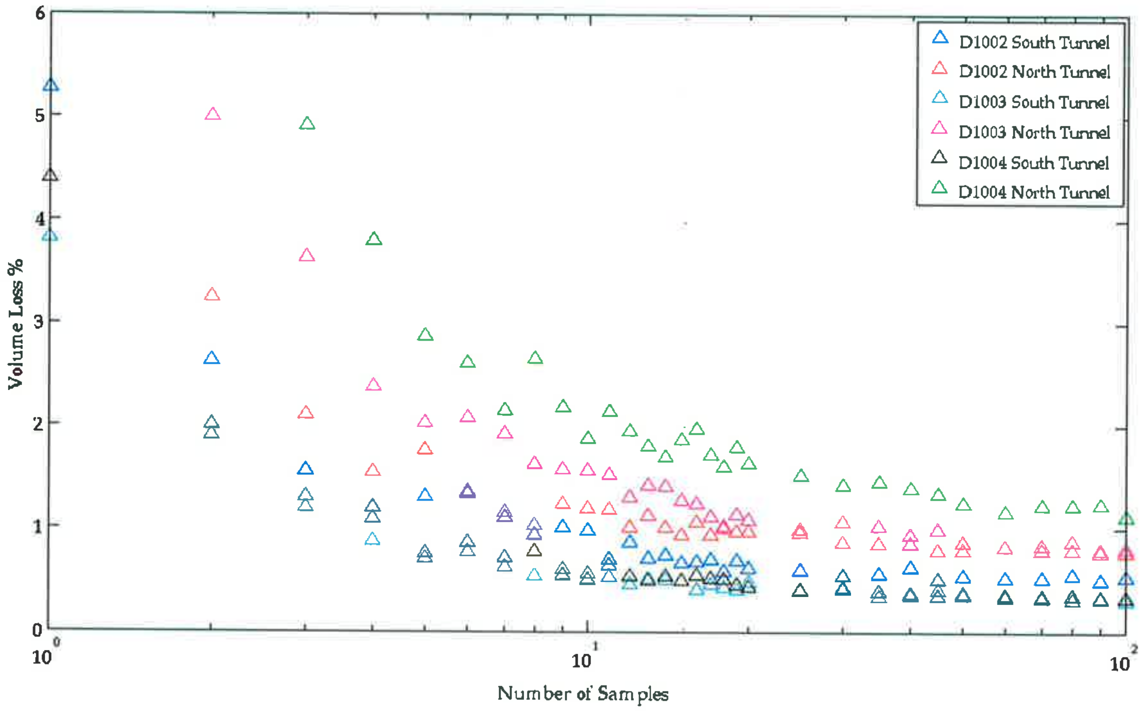

Figure 4-5 - Volume Losses versus Number of Samples

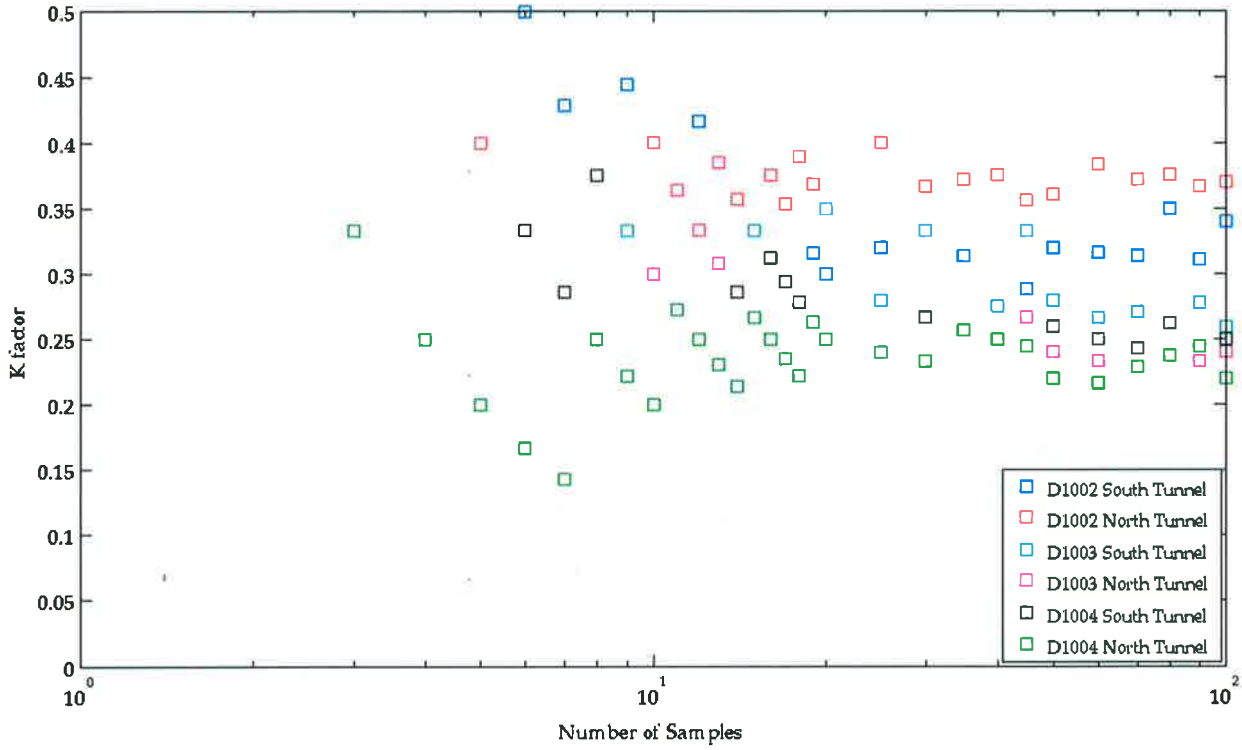

Figure 4-6 - Trough Width Parameter versus Number of Samples

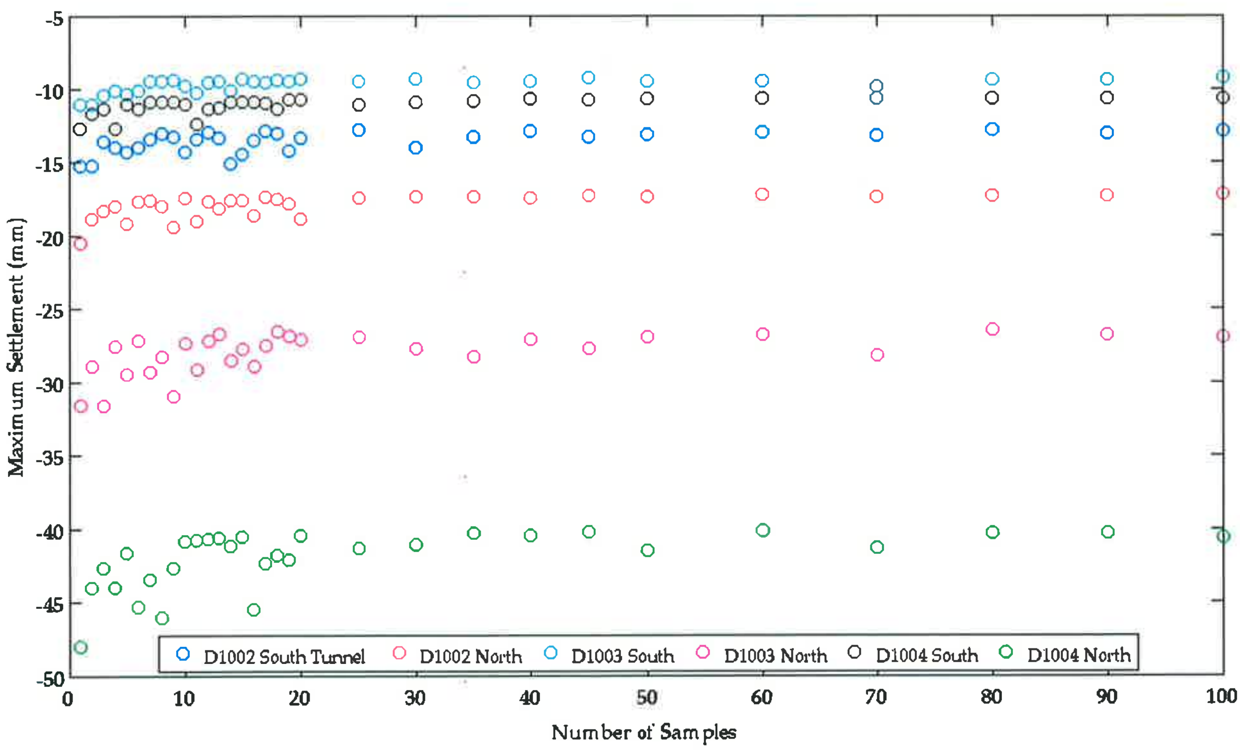

Figure 4-7 - Maximum Settlement versus Number of Samples

5 Ground Investigation Methodology and Results

5.1 D10 Transverse Settlement Investigation

D10 was the first section of tunnel to be constructed shown in Figure 3-3. The wealth of data available means that this section will provide the best engineering knowledge about the ground movements we can expect in similar ground conditions elsewhere in Warsaw. Plotting chainage data from IRIS revealed tunneling progressed at a fairly constant rate of 20m/day on this section, which is significant considering the maximum rate of 2m/day when constructing Line I.

The procedure to produce Figures 5-1 to 5-5 is as follows:

1. MATLAB was used to produce a plot similar to Figure 3.9 for all 63 transverse sets of ground pins.
2. Data was selected at positions 1, 2 and 3 and extracted from global data files to isolate settlement troughs caused by the South and North Tunnels individually. These were stored in a separate Excel file.
3. A MATLAB script imports the data from this file, runs the sweep described in 4.1.4 with N=40 and stores values for V_L, K and Smax in a $63x2$ array (one for the Southern tunnel and one for the Northern)
4. These arrays are separated into soil categories using the geotechnical cross sections, a section of which is shown in Figure 3-10.
5. The 63 data points are plotted against chainage for the North and South tunnels. Chainage values were calculated by running a separate MATLAB script to rotate the North-East coordinates of each settlement point into a plane with an axis parallel to the tunnel using a rotation matrix.

5.1.1 Volume Loss verses Chainage

V_L is calculated using equation 2.2 after each sweep. Values are plotted separately for the south and north tunnels in Figure 5-1 and Figure 5-2. The data is separated based on the majority soil layer found in the cross section of the tunnel face. Admittedly influences other than tunnel face material have a significant effect on V_L, namely the face pressure of the EPB TBM.

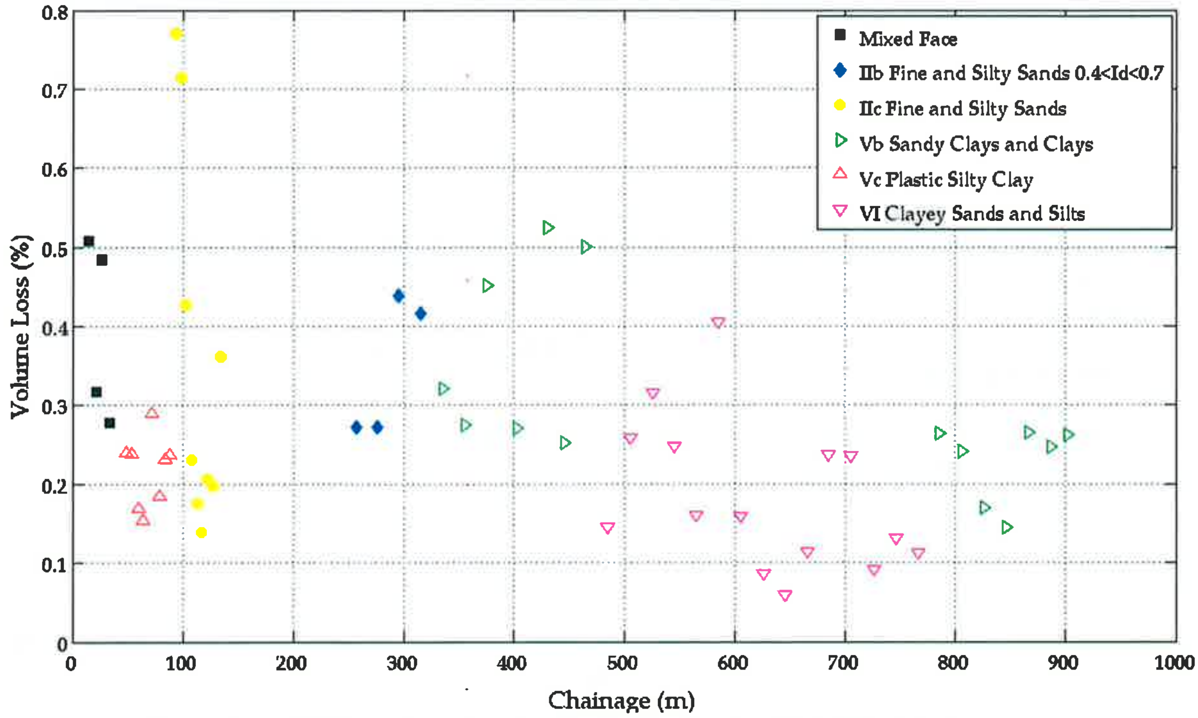

Figure 5-1 - Volume Loss versus Chainage for the First (South) Tunnel

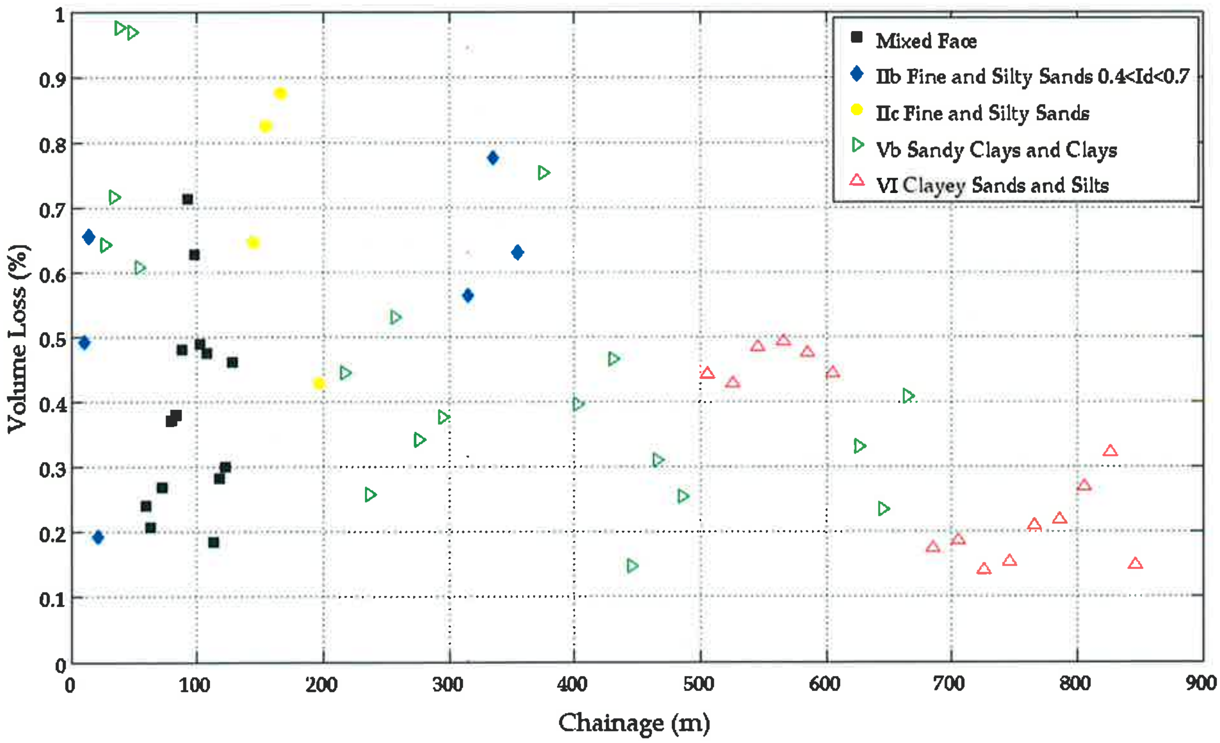

Figure 5-2 - Volume Loss versus Chainage for the Second (North) Tunnel

5.1.2 Trough Width Parameter K verses Chainage

K was also calculated per sweep using equation 2.4 and plotted in Figure 5-3 and 5-4.

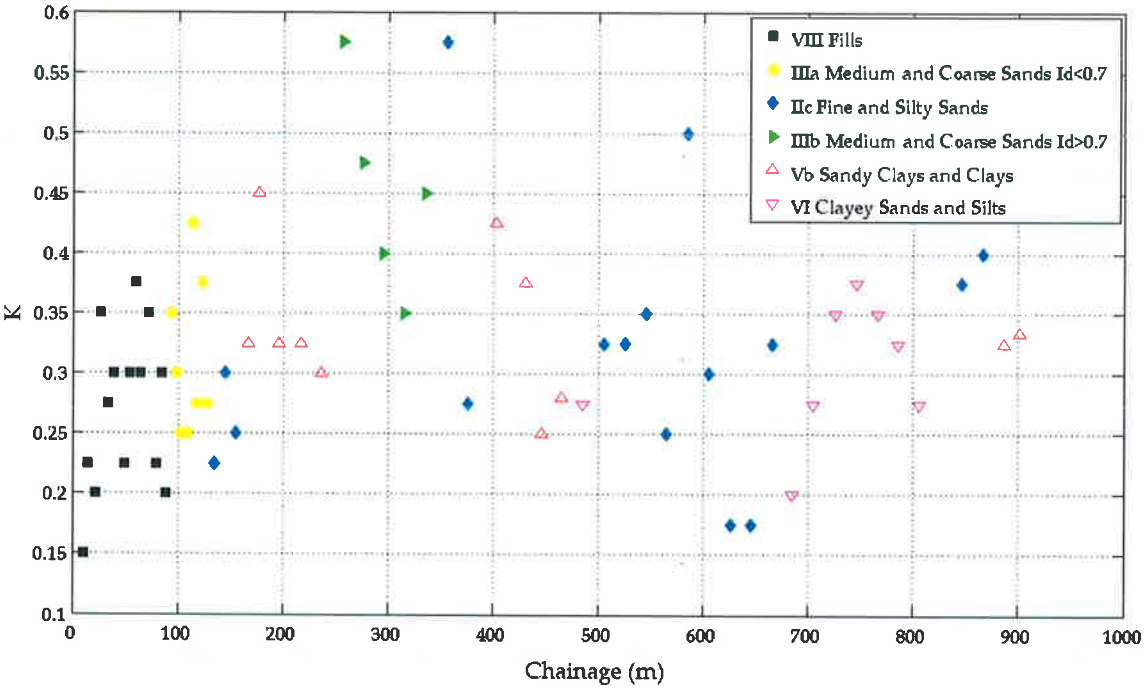

Figure 5-3 - Trough Width Parameter versus Chainage for the First (South) Tunnel

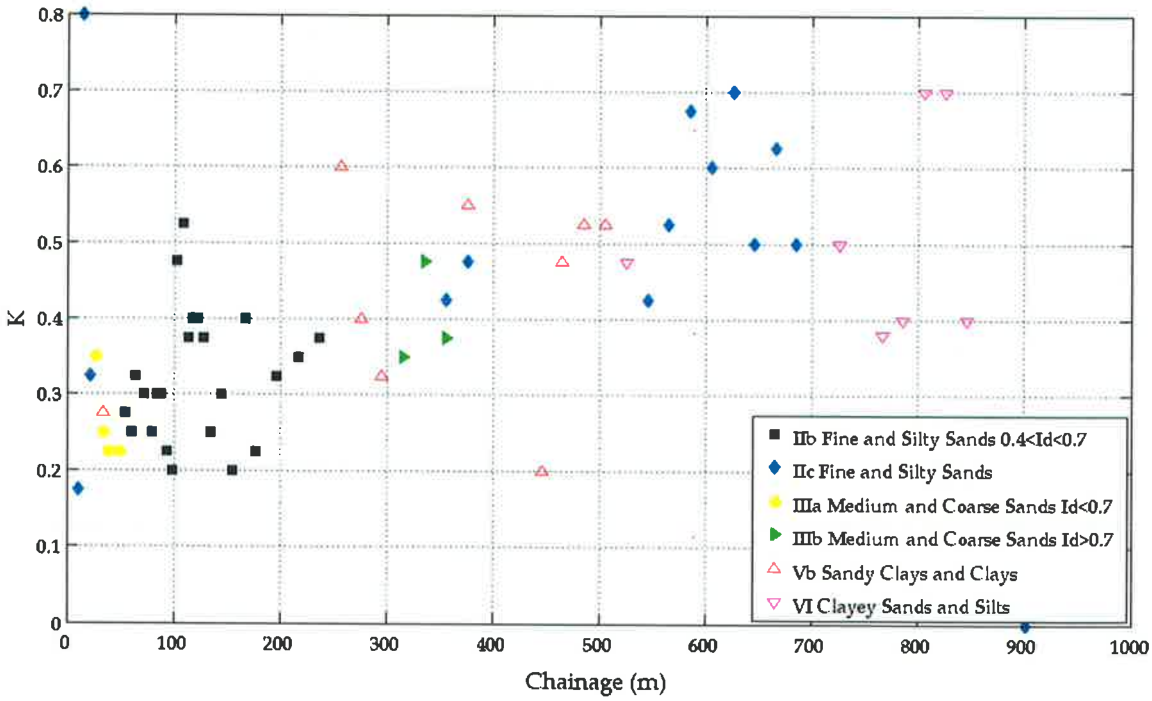

Figure 5-4 - Trough Width Parameter versus Chainage for the Second (North) Tunnel

As K is dependent on tunnel axis depth z_0, this parameter was changed each sweep according to depths measured off the geotechnical cross section. North and South tunnel effects are plotted separately again for clarity. The data is separated here based on the majority soil present between the tunnel's crown and the ground surface. The soils present are non-cohesive sands (IIb, IIc, IIIa and IIIb), cohesive clays (Vb, Vc and VI) and anthropogenic fills VIII as the top layer.

5.1.3 Maximum Settlement *Smax* verses Chainage

Smax was recorded per sweep, not as the maximum measured data point, but the largest value of the approximated Gaussian curve. The values are not grouped into different ground materials and the settlement caused by both the south and north tunnels are plotted in Figure 5-5: One very large initial settlement (-92.8mm) was significantly bigger than the majority of the results so it was omitted from this chart to enable the useful results to be presented clearly. Despite omitting this value here it will not be ignored in the discussion.

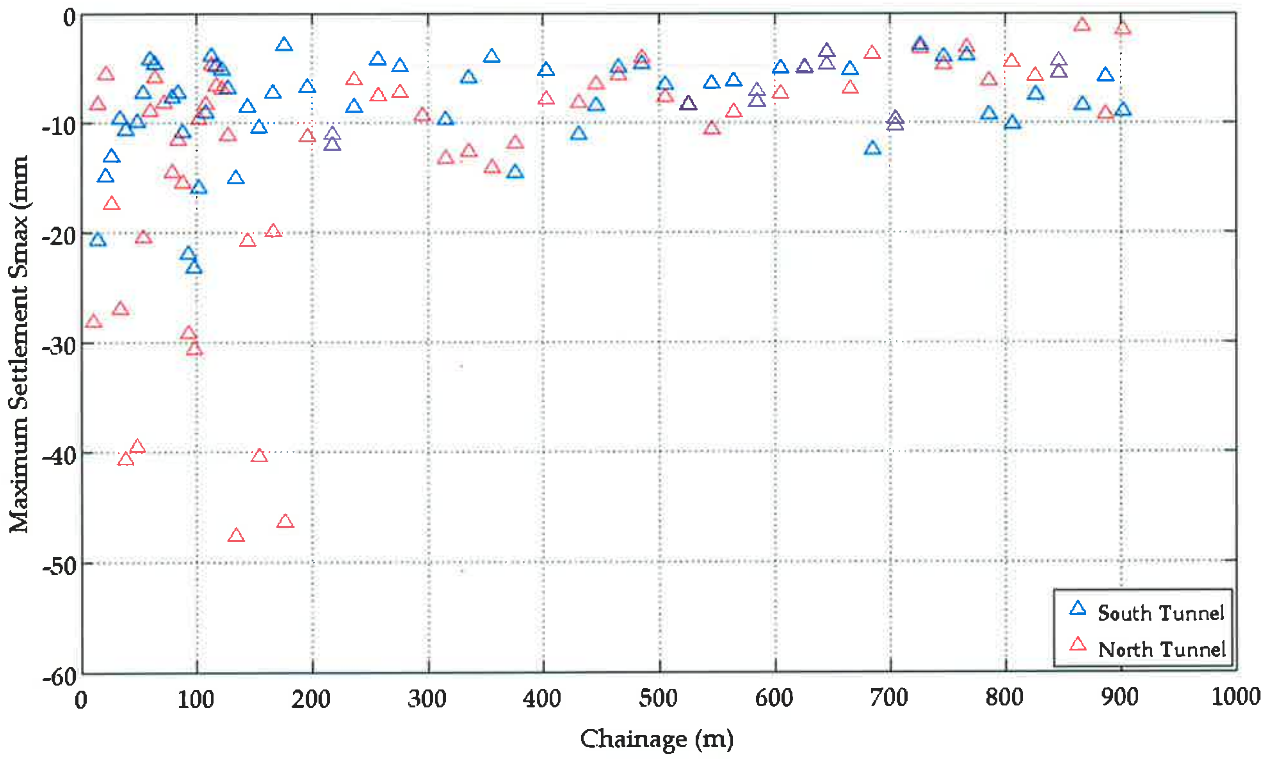

Figure 5-5 - Maximum Settlement versus Chainage

5.2 Line 1 and Grouting Investigation

The primary aim of this investigation was to compare nearby green field ground movements with those directly above Line I. The secondary aim was to investigate the grouting process in terms of volume gained by heaving and volume losses of the grouted region. As this is potentially the most sensitive point of Line II's construction considerable monitoring equipment was installed. The ones chosen for this investigation are indicated in Figure 5-6.

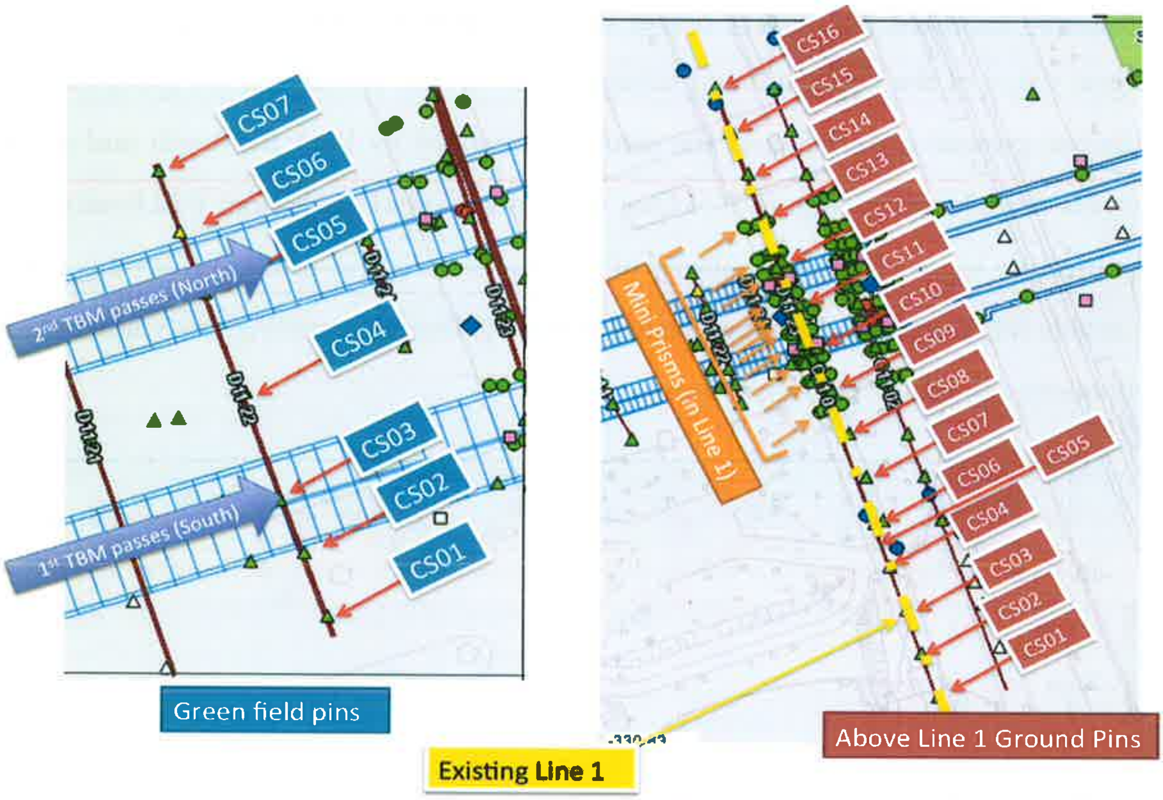

Figure 5-6 - Green Field, Line I Ground Pins and Tunnel Floor Mini Prism Locations

They consist of ground pins (above Line I tunnel and in a greenfield region just outside of the grouted region in Figure 3-6) and mini prisms (situated on the tunnel floor of Line I). Grouting pressure charts were provided however they were not dated so they were disregarded as a useful resource. In order to understand the chronology of the grouting procedure and tunnel construction inspective work was done using Figure 5-7, Figure 5-8 and Figure 5-10.

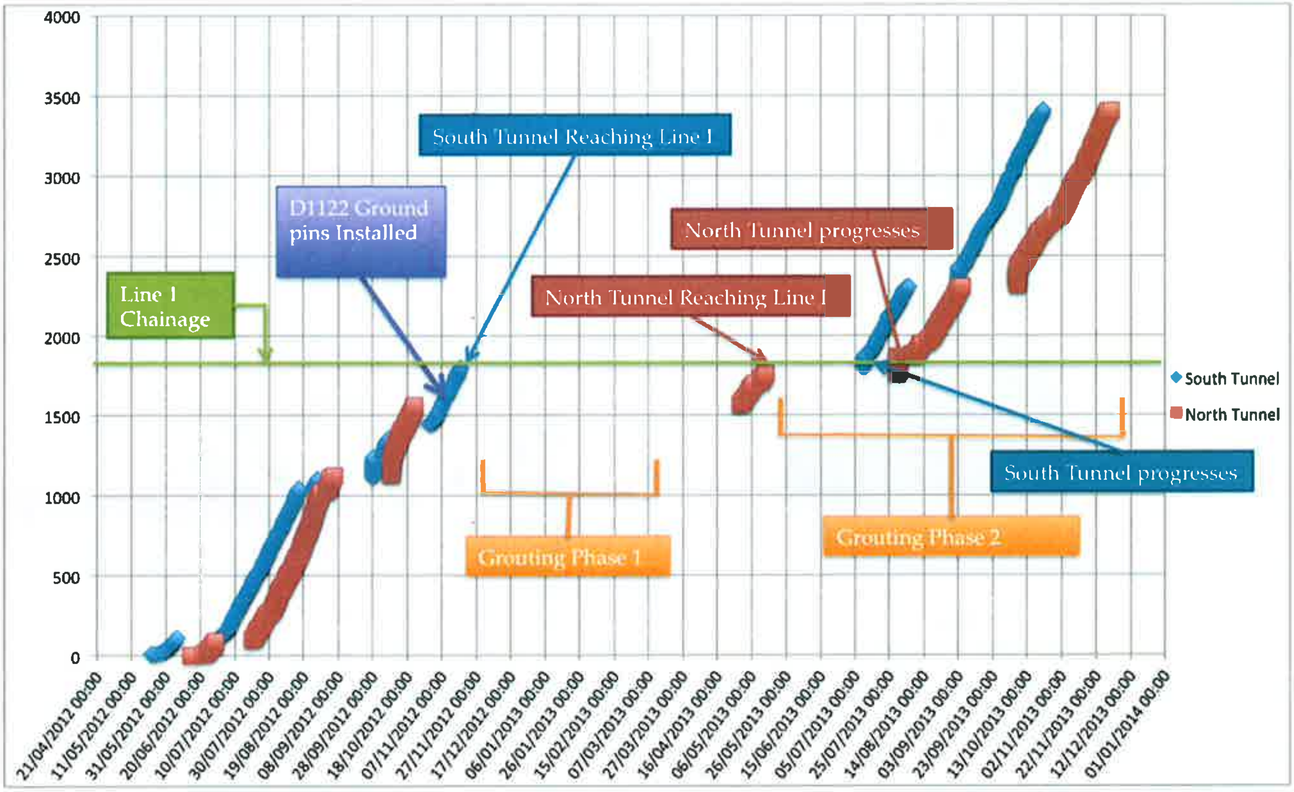

Figure 5-7 - Chainage versus Time for Northern and Southern Tunnels

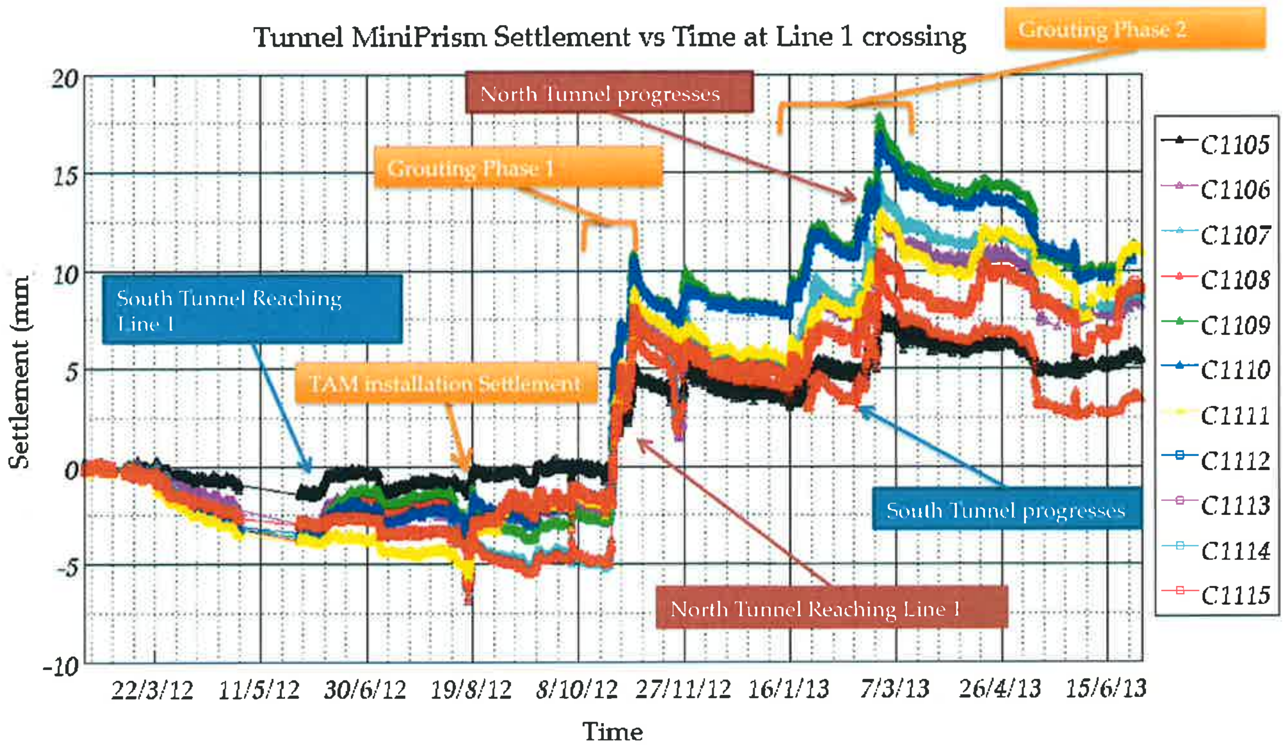

Figure 5-8 - Line I Tunnel Floor Mini Prisms Displacements versus Time

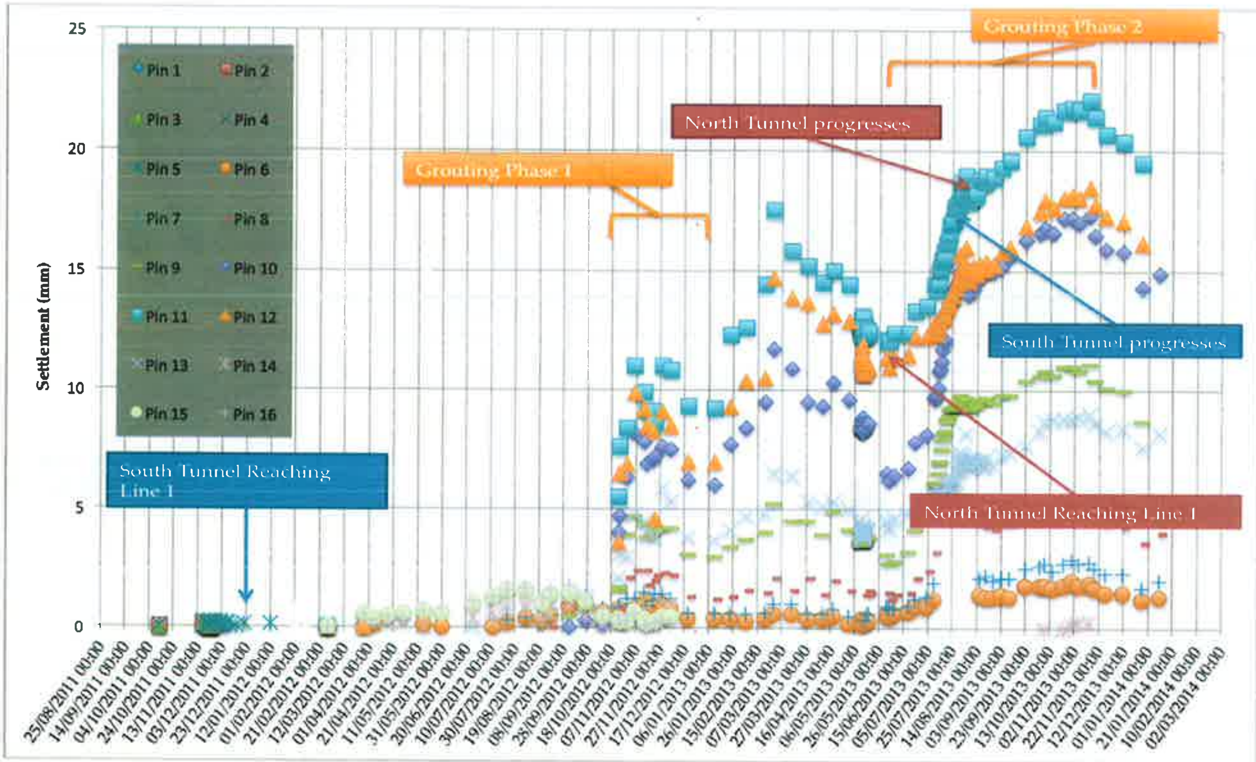

Figure 5-9 - Above Line I Ground Pins Displacements versus Time

A timeline of what appears to happen is as follows:

1. Southern tunnel reaches Line I circa 17/11/2012.
2. A small settlement trough is observed in the tunnel mini prisms circa 19/08/2012 above the north tunnel axis, before the TBM arrives. This is labeled in Figure 5-8 but does not appear in Figure 5-9 suggesting the trough is caused by the drilling and installation of the TAMs. A Gaussian approximation is fitted to this data, producing a fairly insignificant V_L=0.25 and K=0.4.
3. The first phase of grouting takes place. This causes fairly significant heave, observed in both and Figure 5-8 and Figure 5-9. This heave is represented by both the above Line I ground pins and tunnel floor mini prisms in
4. Grouting appears to stop as the Northern tunnel approaches Line I. This appears to cause a settlement trough above the northern tunnel axis in the

tunnel mini prisms. This is plotted along with the above Line I ground pins and the Greenfield ground pins in Figure 5-12.

5. The second phase of grouting begins. During this phase the south tunnel proceeds first, followed shortly after by the north tunnel. Procession of the south tunnel causes little ground movement above Line I (Figure 5-9) but does show some settlement of the tunnel mini prisms (Figure 5-8). This settlement was almost negligible with a maximum value of -1.31mm producing a very small volume loss of V_L=0.07%. The heave caused by this second phase is represented in Figure 5-13.
6. Grouting appears to stop for a final time circa 10/11/2013, by which time the TBMs have travelled over a kilometer beyond Line I. Both the above Line I ground pins and the tunnel mini prisms experience a gradual settlement, potentially due to the 'relaxation' of the grouted soil as stresses dissipate over time and grout pressures are no longer being applied.

All the parameters calculated in this section are summarised in Table 3 in 6.2.

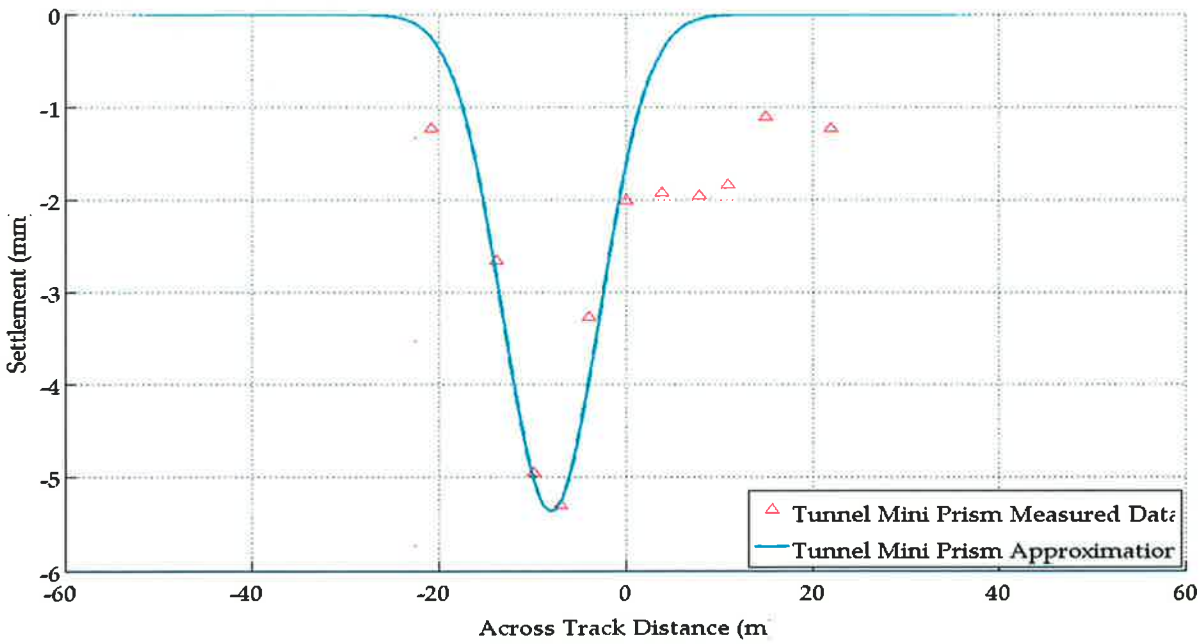

Figure 5-10 - Settlement of Tunnel Floor Mini Prisms Due to TAM Installation

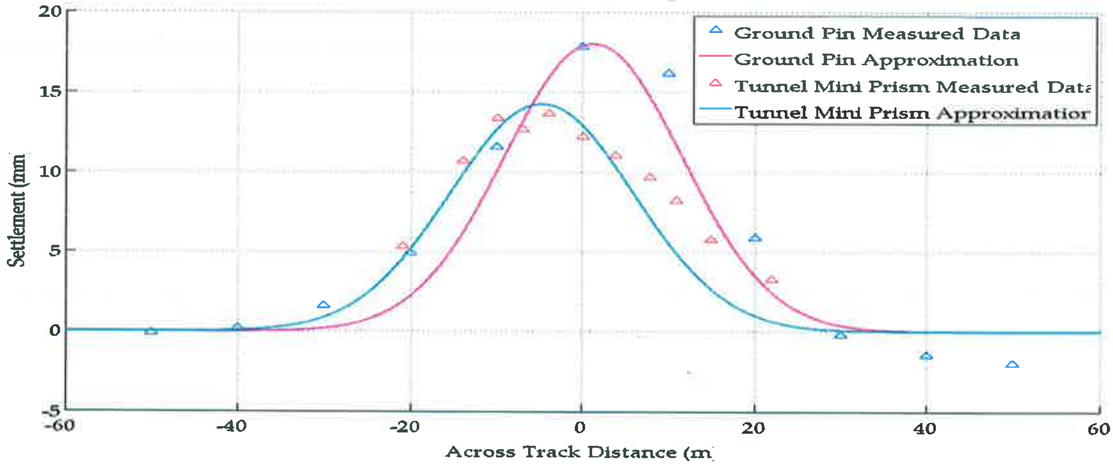

Figure 5-11 - Heave due to Grouting Phase 1

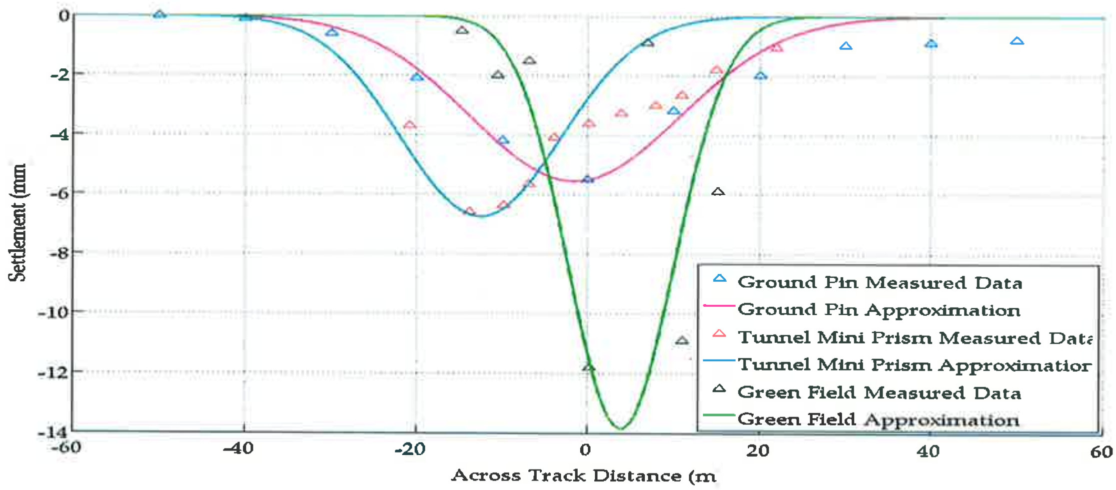

Figure 5-12 – Settlement due to the Arrival of the North TBM

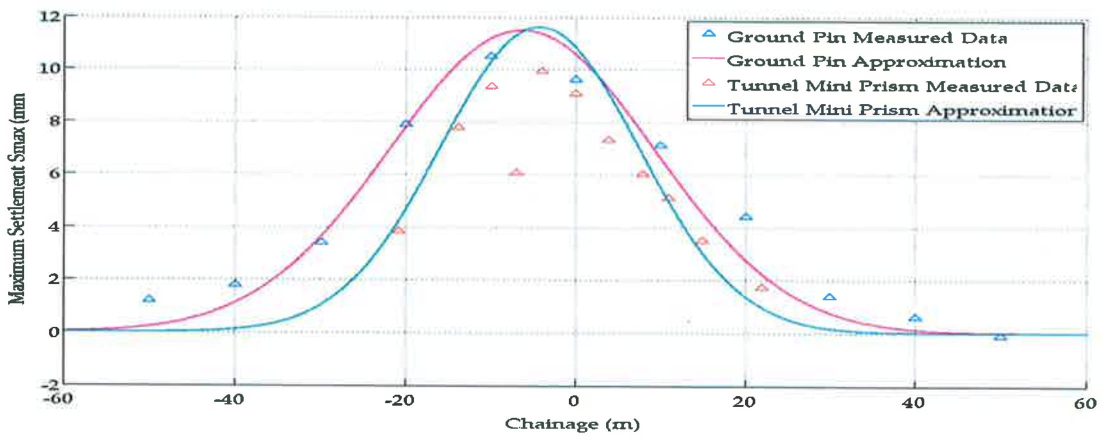

Figure 5-13 – Heave due to Grouting Phase 2

5.3 D13 Building Investigation

Sections D10 and D11 run under the main road Marcina Kasprzaka, a 6-lane dual carriageway. Sections D12 and D13 see the tunnels pass under a number of buildings. As described in section 2.4 buildings can be analysed with respect to their stiffness by comparing their settlement to that of nearby green field settlement. The building to be analysed here is a 5-story masonry structure, around 50m in length situated at the end of the D13 section near to the river. A plan view in Figure 5-14 indicates the green field ground pins and set of mini prisms installed on the building itself.

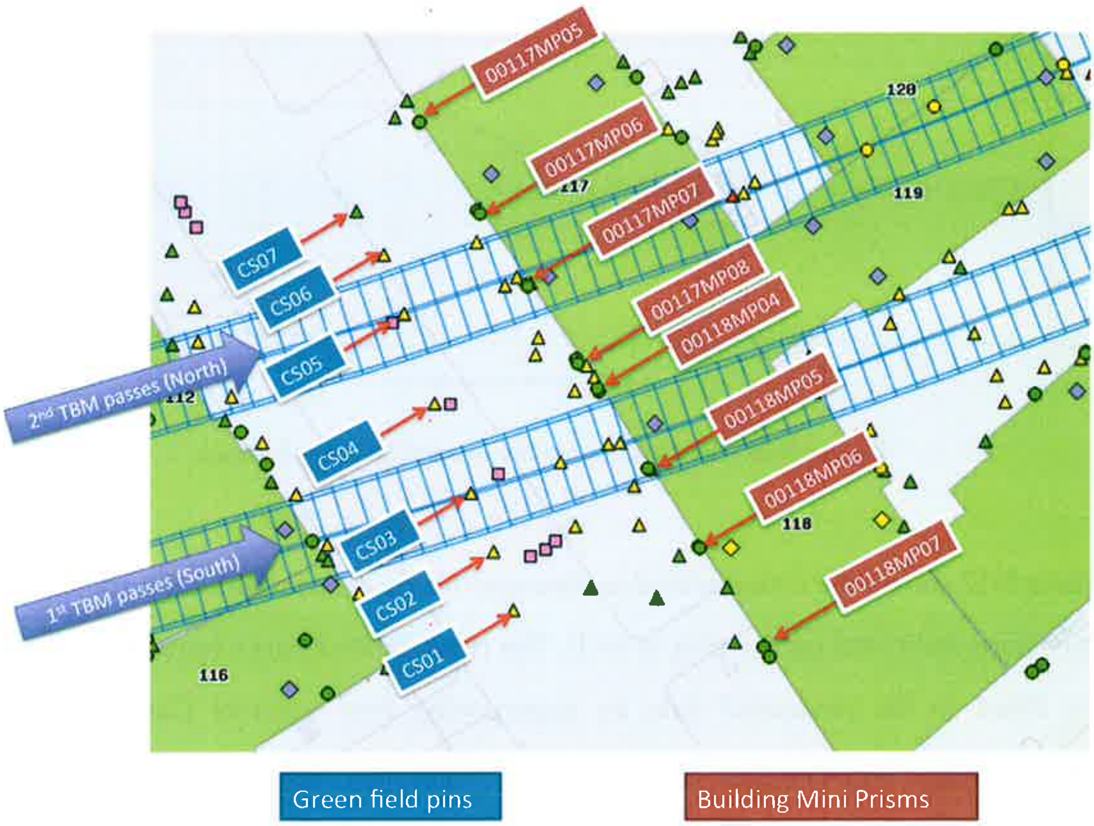

Figure 5-14 - Layout of Green Field Ground Pins and Building Pins

Figures 5-18 and 5-19 indicate the settlement due to the north and south tunnel respectively. It can be seen that the curves are fairly similar indicating that the building is fairly flexible when subject to a single tunnel passing underneath.

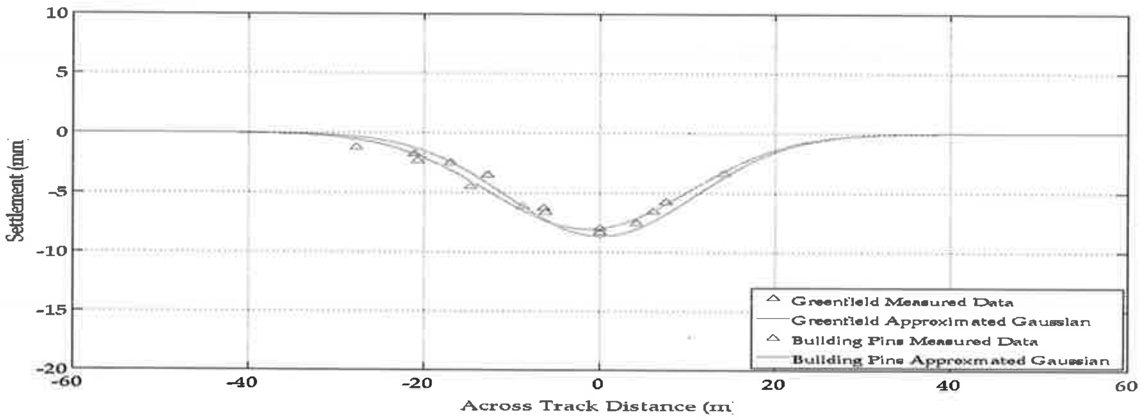

Figure 5-15 - Settlement for the First (South) Tunnel Passing

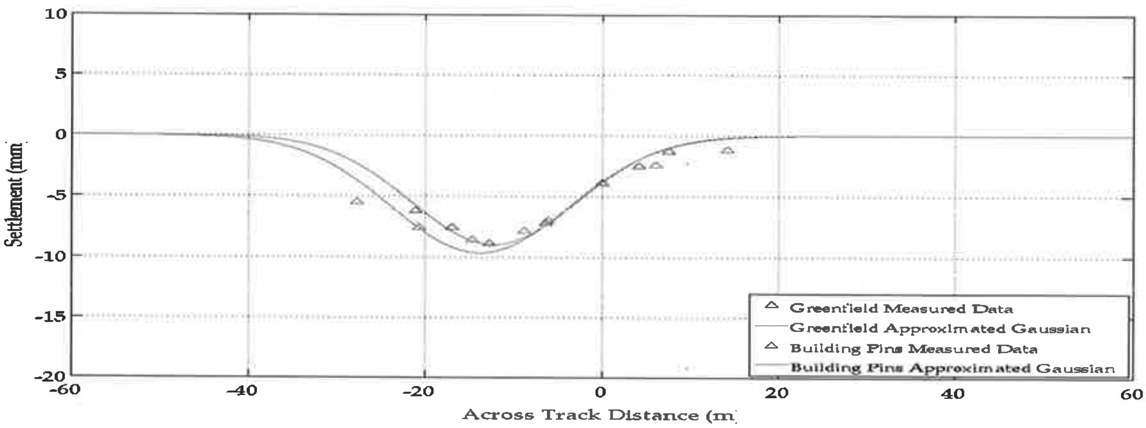

Figure 5-16 – Settlement for the Second (North) Tunnel

Figures 5-17 shows the consolidated settlements for the green field, with the building dimensions indicated on the plot as well. The consolidated curve approximation has been fitted to the measured data by superposing two separate Gaussian curves (Aoyagi, 1995). The building has then been separated into hogging and sagging regions, evaluating $\frac{\Delta}{L}$ for each region to calculate modification factors, as in section 2.4.

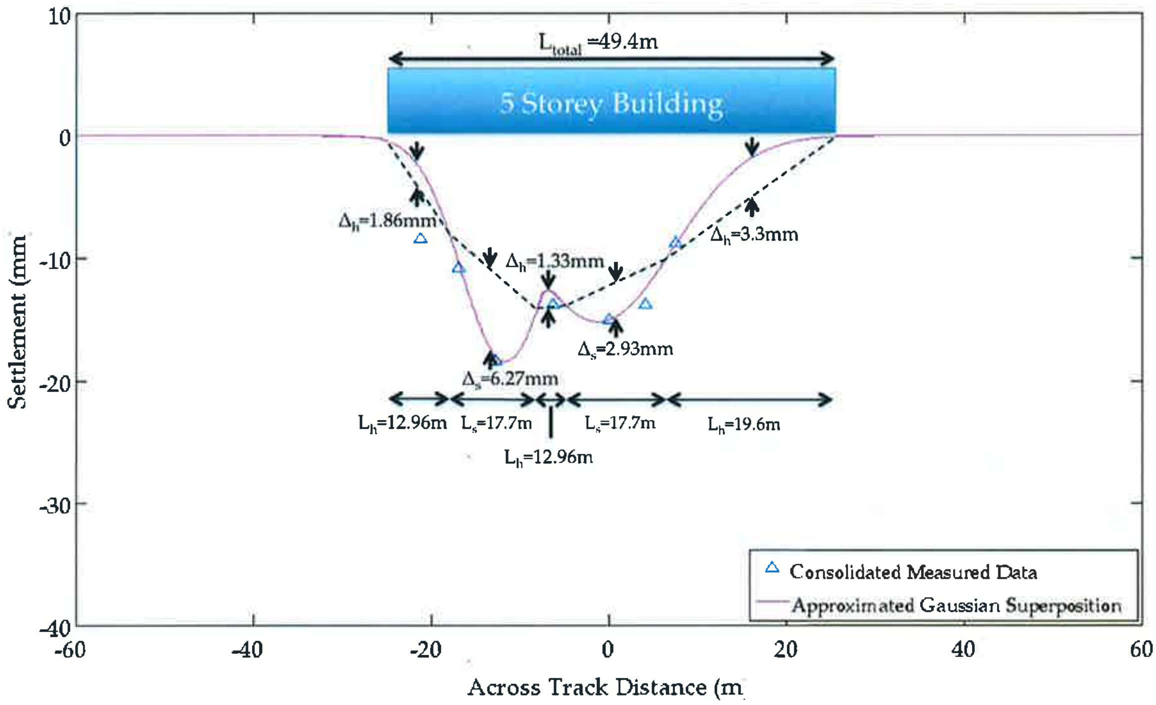

Figure 5-17 - Greenfield Consolidated Settlement Curve

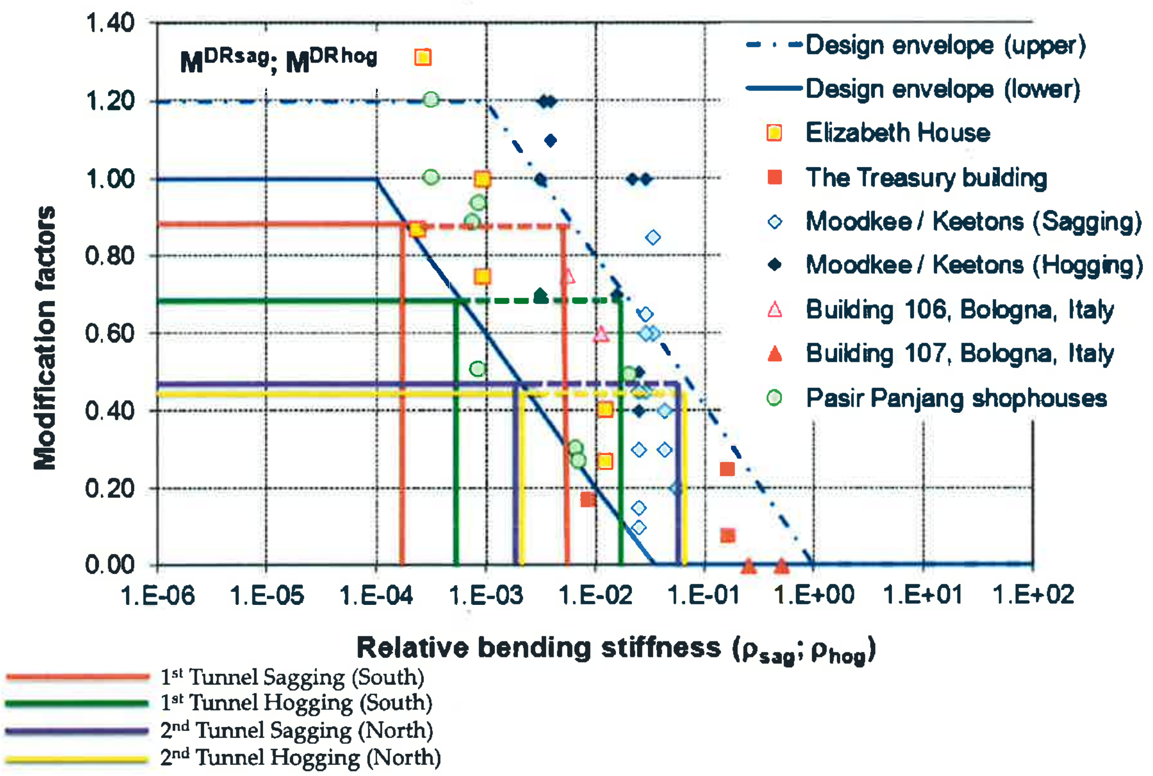

Figure 5-18 - Modification Factor versus Relative Bending Stiffness

6 Discussion

6.1 D10 Transverse Settlement

This investigation successfully brought together the data processing techniques from 3.6 and the Gaussian curve approximation from 4.1.4. Admittedly significant time was devoted to selecting north and south passing settlement troughs for all 63 data sets, but once acquired it was hugely satisfying to leave MATLAB to produce 126 Gaussian approximations automatically. The outcome of this was useful geotechnical engineering parameters for six of the common ground materials found in Warsaw. These parameters are summarised in Table 2 below.

		Volume Loss (%)		Trough Width Parameter	
Soil Layer		South Tunnel	North Tunnel	South Tunnel	North Tunnel
Mixed Face		0.63	0.39	-	-
IIb	Non-Cohesives	0.35	0.55	-	0.32
IIc	Non-Cohesives	0.29	0.87	0.32	0.50
IIIa	Non-Cohesives	-	-	0.31	0.26
IIIb	Non-Cohesives	-	-	0.4	0.45
Vb	Cohesives	0.30	0.48	0.34	0.43
Vc	Cohesives	0.22	-	0.30	0.46
VI	Cohesives	0.18	0.46	-	-
VIII	Cohesives	-	-	0.27	-

Table 2 – Volume Losses and Trough Width Parameters for D10 Transverse Investigation

The values in these tables were provided by taking average values for groups of data represented in Figures 5-1 through 5-4. Certain outliers were ignored when calculating these values such as IIc's K values in Figure 5-4 near the beginning and end of the section as these are clearly anomalous. Some groups also showed significant spread such as IIc's volume losses in Figure 5-1 and the mixed face volume losses in Figure 5-2. These means too must be treated with caution. The very first set of data at 10m chainage produced a large volume loss of 1.6% caused by a maximum settlement of 97.2mm. This point has been omitted from Figure 5-1 to enable the most useful results to be displayed clearly.

There is a general trend concerning volume losses that the second tunnel causes greater volume losses than the first. This is true for all soil layers except the mixed face. Mixed faced conditions can experience higher volume losses for EPB of slurry shields (Mair. 1997) and the categorisation refers to a range of mixed faces in Figures 5-1 and 5-2, accounting for the difference in these values. The usual values for EPB TBM are in the range of 0.3-0.6%, with maximum values of 1% when operating parameters of the TBM are not regulated properly; the lower values of the range are typical of cohesive soils, while the higher values of 0.4-0.6% are expected for granular grounds (Gatti and Cassani 2007). The values for the passing of the first tunnel in non-cohesive soils (IIb and IIc) are as expected, falling at the lower end of the range. This could be as a result of effective parameter control from the tunneling engineers. The values for the second tunnel are slightly larger than those in the expected range but these can be accounted for by the proximity of the first tunnel and its associated ground movements.

Values for the passing of the first tunnel in cohesive soils (Vb, Vc and VI) are again at the low end of the expected range, and slightly less than our non-cohesive values, as expected. At low chainage values, the large volume losses can be accounted for via tunneling inexperience as described by Gatti and Casani, 2007. Experience acquired from this investigation should prevent these occurring for later construction phases.

Volume losses in Table 2 can be used in design of future sections of tunnel, alongside knowledge of the soil layers experienced by the tunnel face.

Trough width parameters too show a general trend that K increases for the second tunnel compared to the first. That is except in soil layer IIIa, however IIIa experiences significant spread in Figure 5-3 such that this average may be a misrepresentation. Values in non-cohesive soils are as would be expected, falling between 0.25-0.45 (O'Reilly and New, 1982). However values for cohesive soils are significantly smaller that expected, anticipating values between 0.4-0.6 (O'Reilly and New, 1982). Some inspiration as to why this may be the case is that Vb is described as sandy clay, which account for its K values being nearer to that of sands. They are both also described as having high probability of pebbles, stones and boulders that may act to reduce the shear strength of the soil. This subsequently produces a narrower settlement trough, and hence smaller K values.

Figure 5-5 shows the maximum settlement due to each tunnel passing against chainage. The primary observation is that it portrays a learning curve (Mair 1996) typical of many tunneling projects during the early stages of construction. This is as the tunneling engineers acquire knowledge from monitoring via feedback loops, improving their understanding of the grounds response to the tunnel passing. This accounts for the very large initial settlement of -92.8 mm caused by the south tunnel passing the first set of ground pins. Disregarding this value we still see a number of significant settlements during the first 200m of chainage, however by 400m there are only a very small number of settlements exceeding 10mm. When constructing future sections of Line II the tunneling engineers ought to maintain this level of precision from the start of the next section.

As mentioned in 5.1.3 the face pressure of the TBM can play a vital part in surface settlement but unfortunately it has not been possible to obtain face pressure information to compare with volume losses for this section. This would provide an interesting further area of research should the information be obtained.

6.2 Line I Under Passing Investigation

Table 3 below summarises the volume losses (or increases) and K values for the different stages described in 5.2. Unfortunately as mentioned in 3.4.1 there are only about 50 data points maximum for the green field ground pins, giving rise to the its limited representation.

	Ground Pins				Mini Prisms	
	Greenfield		Above Line I		Tunnel Floor	
	V_L (%)	K	V_L (%)	K	V_L (%)	K
TAM installation	-	-	-	-	0.25	0.4
Grout Phase 1	-	-	+1.52	0.8	+1.24	0.82
North Tunnel Reaching Line I	0.7	0.47	0.56	0.95	0.52	0.72
Grout Phase 2	-	-	+1.15	1.2	+0.99	0.85
South Tunnel Progressing	-	-	-	-	0.07	0.42
Residual Settlement	-	-	0.28	0.95	0.44	0.57

Table 3 - Summary of V_L and K Values for Line I Investigation

The installation of the TAMs caused fairly isolated settlement of the mini prisms lying above the northern tunnel but minimal settlement of the mini prisms over the southern line, and negligible ground settlement. This means that when using grouting in the future TAM installation should not cause any worries regarding surface settlement, but may need to be considered if there are any subsurface structures such as other tunnels or deep foundations.

The two grouting phases indicate substantial heave, producing 1.52% of the tunnel area at the ground surface due to the first phase and 1.15% due to the second. Interestingly the second phase produces a wider ridge suggesting that the second phase of grouting is more inclined to spread outwards rather than producing further upwards displacement.

As described in 5.2 the chronology of the TBMs arrival and procedure alongside grouting taking place requires substantial inspection. To enable a simpler investigation the tunnels might have perhaps stopped 50m prior to Line I, grouting might have occurred in a single phase above the north tunnel, then the TBMs might've proceeded, like the rest of the line, about a month apart. This would enable the effective comparison between the two tunnels, both past the green field, then through the respective grouted and non-grouted tunnel paths. However Figure 5-7 shows that this is clearly not the case, with the most useful comparison being the settlement due to the arrival of the north tunnel, shown in Figure 5-8 and 5-9.

The inspection does show that the grouting acts to reduce the volume loss of surface settlements from 0.7% to 0.56%. Observing a cross section similar to Figure 3-10 for the D11 section of tunnel reveals that Line I is constructed in a band of high plasticity clay, Ia. This is a less dense soil than the cohesive soils in 6.1 providing a suggestion for the increase in volume losses from those found in D10. Another observation is the increased K value, particularly for the above Line I pins and to a lesser extent with the tunnel floor prisms. This provides strong evidence that grouting above the crown of a tunnel acts to widen the settlement trough caused by the passing of a TBM.

Chainage information reveals that both TBMs undoubtedly progress during the second grouting phase. It can only be assumed that monitoring provided extensive feedback for the grouting process, such that a settlement trough is not observed as either tunnel progress. The rate of increase of heave shown in Figure 5-9 does appear to reduce slightly once the tunnels have progress at circa 05/08/13 before it stops at circa 20/11/13.

The final observation is that the grouted region appears to settle once grouting has ceased, causing a small volume loss at the ground, and a slightly larger one at the tunnel floor. This could be due to grout material continuing to spread as any excess pressure is dissipated. Unfortunately the measured data in Figures 5-8 and 5-9 terminate before it is clear whether or not this relaxation is slowing down and at what settlement it might come to rest. This would be another interesting further investigation to decipher how much grout 'relaxes' once pumping has stopped and what effect this has on the surface settlements in the grouted regions.

6.3 D13 Building investigation

When accessing measured data via ddsmonitoring one observation is the sheer extent of monitoring installed on buildings under which the tunnel is set to travel. This provides scope for many further investigations, similar to the one outlined in 5.3. The products of 5.3's investigation are the modification factors shown below.

	1st Tunnel	2nd Tunnel	Both Tunnels
Hogging	0.699	0.429	0.289
Sagging	0.850	0.456	0.324

Table 4 - Building Investigation Modification Factors

Interestingly the passage of the first tunnel produces the most flexible response from the building, which reduces for the second tunnel, and reduces further again for consolidated effect long after both tunnels have passed. This is an interesting observation as intuition might say that the building would be stiffest originally, becoming more flexible as it deforms and cracks start to open up. One explanation could be that as the ground deforms, treating the building as a beam, the top of the building will be in compression in the sagging zone, which is the largest, central region. If in the non-deformed state, the building has some flexural strain capacity then this will be utilised by the first tunnel passing, followed by the second to a lesser extent. If this flexural strain capacity has reduced then a stiffer response might be expected, as seen in Table 4. Further investigation in this area would be to look at different buildings of varying size, shape and construction material as well as other masonry buildings to verify or dismiss the above theory of stiffness increasing with time.

The modification factors are plotted in Figure 5-18 showing a range of relative building stiffness's for the building's response to the individual tunnels passing. The ranges for the consolidated modification factors have been omitted to provide clarity for the individual tunnel responses, however it is straightforward to obtain a relative building stiffness range for consolidated troughs like the one in Figure 5-17.

6.4 Further Scope for Approximating in Ground Movements

Producing the fully functional approximated curve algorithm in 4.1.4 was a substantial time investment, developing MATLAB skills in the process, and overcoming many unforeseen difficulties that arose from abnormalities in raw data. However the end result, being able to plot reliable 'best-fit' approximations to any set of raw data proved its worth in the methodologies in section 5, particularly in 5.1 where fitting 126 curves by hand would have been a lengthy process. During the investigations in section 5 there were still a number of tasks, which were carried out manually, namely in 5.3. These consisted of superposing 2 separate Gaussian curves to fit consolidated settlement data, finding points of inflection on these curves and deciphering sagging and hogging deflection ratios. Unfortunately there was insufficient time to write MATLAB scripts to perform these tasks within this project. However with them at our disposal, relevant green field and building pin information could be selected for every building along the tunnels path and stored in an Excel file. The code could then be run, providing modification factors automatically for all the buildings on the line. The process for producing these scripts would not be dissimilar to the one described in 4.1.4. For the purpose of further developing these techniques the next two sections give a brief explanation of how they could be achieved.

6.4.1 Superposed Approximation for Consolidated Settlement Curves

This would involve running two physically adjacent sweep processes like that in 4.1.4, summing the two curves and measuring the horizontal and vertical distances from each measured data point, to the summated curve. As long as the adjacent sweeps are calibrated such that the region of measured data is sufficiently swept with a close enough mesh then a best-fit superposed curve could be found by minimising d as in 4.1.4.

6.4.2 Deflection ratio automated calculation

The superposed curve above can be assigned a function based on the two Gaussian curves that are summed to produce it. This function could then be differentiated twice to locate the positions of the points of inflexions. Connecting these points with straight lines, and to the points on the curve underneath the edge of the building will define the hogging and sagging regions for a particular building. If each of these straight lines is also assigned a function then another simple sweep process could determine the maximum distance between these lines and the consolidated curve for each separate region. Finally the maximum hogging and sagging deflection ratios could be selected to calculate modification factors using the theory in section 0.

6.5 Final Consideration for MATLAB Modeling in Tunneling Construction Feedback Loops

Realisation of just how much settlement data is taken during construction alongside how much useful information can be taken from a simple Gaussian approximation led to believing that real time approximations of measured settlement data could play an important part in the monitoring feedback loops employed during construction. For example rather than simply monitoring the maximum settlement of high priority pins, making sure they remain below threshold values, analysis could be done in real time using powerful computers which could place a building as a live data point on a building damage category chart (Mair, Taylor and Burland, 1996) for example. This is just one application of how approximated information could be used in feedback loops, but there are certainly a host of avenues that could be pursued as a continuation of the work undertaken in this project.

7 Conclusions

This project has developed an effective methodology of analysing monitoring data which has been applied to real field data obtained during the construction of the second Metro line in Warsaw. MATLAB has been utilised in data processing techniques and solving algorithms to provide fit Gaussian curves to the measured data. These enabled useful geotechnical engineering parameters to be obtained for the common soil layers in Warsaw, which corresponded with expected values from literature. Grouting techniques were investigated, showing a reduction in volume loss and an increase in trough width parameter for grouted regions compared to nearby green field. Building stiffness was investigated, revealing that masonry buildings increase in stiffness from the second tunnel compared with the first, and furthermore for the consolidated case. Finally consideration was provided as to how the MATLAB techniques could be further developed, enabling greater automation of analytical techniques that could be integrated into more intelligent monitoring feedback systems.

8 References

Aoyagi, Takahiro. 1995. 'Representing Settlement For Soft Ground Tunneling'.

Attewell, Peter B, John Yeates, and Alan R Selby. 1986. 'Soil Movements Induced By Tunnelling And Their Effects On Pipelines And Structures'.

Brighthub Engineering,. 2012. 'What Is Geotechnical Engineering?'. Accessed May 19 2014. http://www.brighthubengineering.com/geotechnical-engineering/42482-fundamentals-of-geotechnical-engineering/.

Cassani, Giovanna, and Andrzej Stanczyk. 2012. 'TBM Tunnels - Soil Improvement For TBM Passage Under I Metro Line'. Warsaw: Rocksoil - Advice and Technical Assistance in the Geoengineering Field.

Ddsmonitoring.com,. 2014. 'Monitoring Data Dissemination System'. Accessed May 21. http://www.ddsmonitoring.com/index.php.

Gatti, MC, and G Cassani. 2007. 'Ground Loss Control In EPB TBM Tunnel Excavation'. *Underground Space--The 4Th Dimension Of Metropolises. Taylor And Francis Group, London.*

Geoteko Geotechnical Consultants Ltd.,. 2010. 'Geotechnical Documentation For The Underground Line II In Warsaw From "Rondo Daszynskiego Station" To "Dworzec Wilenski Station" D10'. Representative Of Contractor Of The Central Part Of The Underground Line II In Warsaw. Warsaw: Consortium - Astaldi.

Iris.itc-5.com,. 1992. 'IRIS: Navigation View'. Accessed May 21 2014. http://iris.itc-5.com/WarsawMetroLine2/form_NavigationView.html.

Leica-geosystems.co.uk,. 2010. 'Leica TM30 - Monitoring Sensor - Every Half Second Counts - Leica Geosystems - United Kingdom'. Accessed May 22 2014. http://www.leica-geosystems.co.uk/en/Leica-TM30_77983.htm.

Lejk, Jerzy. 2012. '2012 Annual Report'. Warsaw, Poland.

Macklin, SR. 1999. 'The Prediction Of Volume Loss Due To Tunnelling In Overconsolidated Clay Based On Heading Geometry And Stability Number'. *Ground Engineering* 32 (4): 30--33.

Mair, R.J. 2013. 'Tunnelling And Deep Excavations: Ground Movements And Their Effects'.*Proceedings Of The 15Th European Conference On Soil Mechanics And Geotechnical Engineering - Geotechnics Of Hard Soils* Weak Rocks (Part 4): 51-65.

Mair, R.J., R.N. Taylor, and J.B. Burland. 1996. 'Prediction Of Ground Movements And Assessment Of Risk Of Building Damage Due To Bored Tunnelling'. Geotechnical Aspects Of Underground Construction. Rotterdam: Balkema.

Mair, RJ. 1996. 'General Report On Settlement Effects Of Bored Tunnels', 43--53.

Marshall, AM, Rp Farrell, A Klar, and R Mair. 2012. 'Tunnels In Sands: The Effect Of Size, Depth And Volume Loss On Greenfield Displacements'. *Geotechnique* 62 (5): 385.

Mathworks.co.uk,. 1994. 'MATLAB Documentation - Mathworks United Kingdom'. Accessed May 22 2014. http://www.mathworks.co.uk/help/matlab/.

O'reilly, MP, and BM New. 1982. 'Settlements Above Tunnels In The United Kingdom-Their Magnitude And Prediction'.

Peck, R.B. 2014. 'Deep Excavations And Tunnelling In Soft Ground'. SOA Report. Mexico City: State of the Art Volume.

Railway-technology.com,. 2008. 'Warsaw Metro - Railway Technology'. Accessed May 19 2014. http://www.railway-technology.com/projects/warsawmetro/.

Whalen, Charles T. 1979. 'Control Levelling'. NOAA Technical Report NOS. Rockville: National Oceanic and Atmospheric Administration.

Wikipedia,. 2014. 'Warsaw Metro'. Accessed May 19 2014. http://en.wikipedia.org/wiki/Warsaw_Metro.

9 Appendices

9.1 Risk Assessment Retrospective

The risk assessment conducted at the start of the project proved to be adequate. No extra safety considerations were required on top of the health risks associated with overuse of computer stations. Regular breaks were had and information was displayed with suitable clarity to avoid over straining the eyes during prolonged data analysis sessions.

9.2 Acknowledgements

Thanks to Professor Robert Mair for supervising this project alongside Chris Menkiti at Geotechnic Consulting Group (GCG). Thanks also to Jen Flack, PA to Professor Mair for organising our meetings and to Tim Love for his MATLAB expertise.